

Effects of microtopography to the emissions and carbon isotope ratios of  
methane at Siikaneva, a south boreal mire complex in Finland

Minja Seitsamo-Ryynänen

22.11.2016

Master's thesis

DEPARTMENT OF GEOSCIENCE AND GEOGRAPHY

UNIVERSITY OF HELSINKI

Tiedekunta/Osasto Fakultet/Sektion – Faculty Faculty of Science		Laitos/Institution – Department Department of Geosciences and Geography	
Tekijä/Författare – Author Minja Seitsamo-Ryynänen			
Työn nimi / Arbetets titel – Title The effect of microtopography to methane emissions and to related stable carbon isotopes at Siikaneva, a south boreal mire complex in Finland			
Oppiaine /Läroämne – Subject Geology / Geochemistry and environmental geology			
Työn laji/Arbetets art – Level Master's thesis	Aika/Datum – Month and year 11/12	Sivumäärä/ Sidoantal – Number of pages 60	
Tiivistelmä/Referat – Abstract			
<p>The northern peatlands are significant sources of methane into the atmosphere. As methane (CH<sub>4</sub>) is a powerful greenhouse gas, understanding the mechanics of peatland CH<sub>4</sub> production/consumption and the controls on CH<sub>4</sub> emissions are vital in order to calculate global CH<sub>4</sub> budgets. The isotopic composition of CH<sub>4</sub> can be used as a tool to identify pathways of methanogenesis, CH<sub>4</sub> oxidation and transport.</p> <p>The aim was to learn how microtopography effects CH<sub>4</sub> emission and its δ<sup>13</sup>C values at a boreal mire complex Siikaneva, located in southern Finland. The study sites were an ombrotrophic bog and a minerotrophic fen. The hypothesis of the study was that microtopography is an integrating controlling factor of CH<sub>4</sub> emissions and that isotopic composition of the emitted CH<sub>4</sub> would reflect the processes beneath the peat surface. Also, it was expected that at the fen there would be more acetate fermentation which would show in the isotope results.</p> <p>Gas samples of emitted CH<sub>4</sub> were drawn from hummocks, lawns and hollows using a closed chamber method to analyse CH<sub>4</sub> flux and δ<sup>13</sup>C<sub>CH<sub>4</sub></sub>. Pore water samples for DIC analysis were collected at the depth of 0.5 m to analyse δ<sup>13</sup>C<sub>DIC</sub>. In addition, water table levels and peat temperatures were measured at each sampled plot. All samples were collected once a month from May to August to identify changes during the growing period in 2015.</p> <p>The results revealed that the emissions of CH<sub>4</sub> were the lowest from the hummocks at both sites, but the differences between fluxes from the hollows and lawns were less affected by microtopography. Water table levels and peat temperatures seem not to be the controlling factors for CH<sub>4</sub> emissions. The isotopic composition of emitted CH<sub>4</sub> was also mostly unaffected by microtopography. Only the hummocks at the bog had distinctively higher carbon isotope values compared to the other microsites. Unlike the CH<sub>4</sub> flux results, the δ<sup>13</sup>C<sub>CH<sub>4</sub></sub> results depicted a seasonal trend during the growing period with all the microsites showing the most negative values in July. Combined to the results of the DIC analyses, it appears that the fen is characterized by more acetate fermentation, though the production pathway could not be identified unambiguously.</p> <p>The isotopic composition of emitted CH<sub>4</sub> proved to be a suitable, but not sufficient application to differentiate CH<sub>4</sub> production pathways, oxidation and transport. To better understand the processes beneath the peat surface and the effects of microtopography, CH<sub>4</sub> flux and isotope data should be combined to multi-isotopic (CH<sub>4</sub> and DIC) pore water samples drawn from multiple depths to demonstrate the vertical changes in the isotope composition at different layers of peat.</p>			
Avainsanat – Nyckelord – Key words Methane, stable isotopes, peatland, Siikaneva			
Säilytyspaikka – Förvaringställe – Where deposited University of Helsinki, Department of Geosciences and Geography			
Muita tietoja – Övriga uppgifter – Additional information			

Tiedekunta/Osasto Fakultet/Sektion – Faculty Matemaattis-luonnontieteellinen tiedekunta		Laitos/Institution – Department Geotieteiden ja maantieteen laitos	
Tekijä/Författare – Author Minja Seitsamo-Ryynänen			
Työn nimi / Arbetets titel – Title Mikrotopografian vaikutus suon metaanipäästöjen suuruuteen ja stabiiliin hiilen isotooppikoostumukseen Siikanevalla			
Oppiaine / Läroämne – Subject Geologia / Geokemia ja ympäristögeologia			
Työn laji/Arbetets art – Level Pro gradu -tutkielma	Aika/Datum – Month and year 11/12	Sivumäärä/ Sidoantal – Number of pages 60	
Tiivistelmä/Referat – Abstract			
<p>Pohjoiset suot ovat merkittävä lähde ilmakehään päätyvälle metaanille. Metaani (CH<sub>4</sub>) on merkittävä kasvihuonekaasu ja sitä tuottavien reaktioiden ymmärtäminen on tärkeää muodostettaessa globaaleja metaanitaseita. Metaanin isotooppikoostumusta voidaan käyttää työkaluna tunnistamaan keskeisimmät metaania tuottavat reaktiot.</p> <p>Tutkimuksen tarkoituksena oli selvittää mikrotopografian vaikutus metaanin kaasuvirtojen suuruuteen ja niiden isotooppikoostumukseen kahdella eri suotyypillä, ombrotrofisella keidassuolla sekä minerotrofisella aapasuolla, jotka ovat osa Siikanevan suokompleksia. Lähtöoletuksena oli, että mikrotopografia selittää kaasuvirtojen vaihtelun suotyypien eri pintatyypeillä. Lisäksi oletettiin, että metaanin isotooppikoostumus osoittaa vallitsevan metaania tuottavan prosessin eri pintatyypeillä. Oletuksena myös oli, että minerotrofisella aapasuolla isotooppitulokset heijastaisivat asetaattikäymisen suurempaa osuutta metaania tuottavana prosessina kuin ombrotrofisella keidassuolla.</p> <p>Metaanin kaasunäytteet kerättiin suljetun kammion menetelmällä, ja niistä analysoitiin kaasuvirrat ja hiilen stabiilien isotooppien koostumus. Tutkittavat pintatyypit olivat kuljut, välipinnat ja mättäät. Kammiomittauksen lisäksi veden pinnan korkeus ja turpeen lämpötila mitattiin jokaiselta mitattavalta pinnalta. Puolen metrin syvyydestä kerättiin huokosvesinäytteitä DIC-analyysia varten. Näytteet kerättiin kuukauden välein kasvukaudella 2015.</p> <p>Tulokset osoittivat, että mikrotopografian vaikutus metaanin kaasuvirtoihin oli vain osittainen molemmilla suotyypeillä, sillä vain mättäät erottuivat muista pintatyypeistä selvästi pienemmällä päästöillä. Vedenpinnan tasolla ja turpeen lämpötilalla ei ollut kontrolloivaa vaikutusta kaasuvirtojen suuruuteen kummallakaan suotyypillä. Mikrotopografialla ei myöskään ollut selvää vaikutusta metaanin isotooppituloksiin, sillä vain keidassuon mättäät erottuivat selvästi muista pintatyypeistä korkeammilla hiilen isotooppiarvoilla. Toisin kuin metaanin kaasuvirroilla, isotooppituloksissa on havaittavissa selkeä kasvukauden aikainen muutostrendi. Vaikka vallitsevaa metaania tuottavaa prosessia ei pystytty selvittämään yksiselitteisesti, DIC-tulokset yhdessä kaasuvirtojen isotooppitulosten kanssa viittasivat aapasuon suosivan enemmän asetaattikäymistä kuin keidassuon, jonka tulokset osin viittasivat myös hiilidioksidin pelkistymiseen vallitsevana prosessina.</p> <p>Metaanin kaasuvirran isotooppikoostumuksen selvittäminen on toimiva, mutta yksinään riittämätön työkalu selvittämään vallitsevan metaania tuottavan prosessin. Kaasuvirtojen lisäksi tulisi tutkia eri syvyyksiltä huokosvedeen liuenneet hiilyyhdisteet (CH<sub>4</sub> ja DIC) ja niiden isotooppikoostumukset, jotta havaittaisiin vaihtelut turpeen syvyysprofiilissa ja pystyttäisiin rakentamaan kokonaiskuva metaanin tuottoon, kuljetukseen ja hapetukseen vaikuttavista prosesseista turpeen eri osissa ja eri pintatyypeillä.</p>			
Avainsanat – Nyckelord – Keyw ords Metaani, stabiilit isotoopit, suo, Siikaneva			
Säilytyspaikka – Förvaringställe – Where deposited Helsingin yliopisto, Geotieteiden ja maantieteen laitos			
Muita tietoja – Övriga uppgifter – Additional information			

## CONTENTS

1. INTRODUCTION .....	4
1.1. Methane in the climate system .....	4
1.2. Methane in northern peatlands .....	5
1.3. Isotopic signatures as tools to understand methane production pathways .....	8
1.4. Aims of the study and the main hypothesis .....	10
2. STUDY AREA .....	11
2.1. Geological setting .....	11
2.2. Study sites .....	13
2.3. Weather conditions .....	14
3. MATERIALS .....	16
3.1. Methane concentration samples .....	16
3.2. Methane isotope samples .....	18
3.3. DIC samples .....	18
3.4. Other measurements .....	19
4. METHODS .....	19
4.1. Methane concentration and flux .....	19
4.2. Stable isotope analysis of methane .....	20
4.3. DIC analysis .....	26
4.4. Sources of error and uncertainty .....	26
5. RESULTS .....	28
5.1. Methane flux results .....	28
5.2. Isotope results of emitted methane .....	35
5.3. The isotopes of DIC .....	41
6. DISCUSSION .....	43
6.1. Effects of microtopography on methane emissions .....	43
6.2. Isotopic evidence on methane production, transport and oxidation .....	50
6.3. DIC as an additional tool to identify methane production pathways .....	53
7. CONCLUSIONS .....	55
8. ACKNOWLEDGEMENTS .....	56
9. REFERENCES .....	57

## APPENDICES

Appendix 1	Average fluxes in relation to average $\delta^{13}\text{C}_{\text{CH}_4}$ values at both sites.
Appendix 2	The Keeling plots for both sites depicting all isotope results.
Appendix 3	Mean $\delta^{13}\text{C}$ source signature and flux measurements of each microsite.

## 1. INTRODUCTION

### 1.1. Methane in the climate system

Methane ( $\text{CH}_4$ ) is the third most abundant greenhouse gas in the Earth's atmosphere after water vapour ( $\text{H}_2\text{O}$ ) and carbon dioxide ( $\text{CO}_2$ ).  $\text{CH}_4$  is the most abundant hydrocarbon in the atmosphere, and although its lifetime in the atmosphere is much shorter than  $\text{CO}_2$ , it is much more efficient in trapping radiation than  $\text{CO}_2$ .

Methane's ability to trap heat in the atmosphere (a.k.a. global warming potential, GWP) is 84 times that of  $\text{CO}_2$ , based on a 20-year time horizon and 36 based on a 100-year time horizon (IPCC 2013). This makes it a significant greenhouse gas and an important contributor to global warming. Studies indicate that variations in atmospheric  $\text{CH}_4$  concentrations are closely linked to records of past temperatures (e.g. Chappellaz et al. 1990, Petit et al. 1999, Loulergue et al. 2008), and that increasing  $\text{CH}_4$  concentration will cause global temperature to increase (Lashof and Ahuja 1990).

The atmospheric  $\text{CH}_4$  concentration is a sum of global sources and sinks of methane. The present global concentration of the atmospheric  $\text{CH}_4$  is approx. 1.8 ppm and has increased by a factor of 2.5 since pre-industrial times (IPCC 2013). The globally averaged growth rate of atmospheric  $\text{CH}_4$  had a declining trend from mid-1980s until 2006. Since the beginning of 2007 the growth rate has been observed to increase again (Rigby et al. 2008) and the reason behind it is still unclear. Variations in the growth rate have been linked to climate sensitivity of  $\text{CH}_4$  emissions from natural sources (Dlugokencky et al. 2009) which are the main drivers of the global inter-annual variability of  $\text{CH}_4$  emissions (IPCC 2013).

Globally emitted  $\text{CH}_4$  is a combination of methane derived from naturally occurring sources and anthropogenic inputs. 35 to 50 % of the mean global emissions are from natural sources (IPCC 2013).  $\text{CH}_4$  production processes are either biogenic or abiogenic. Abiogenic  $\text{CH}_4$  is derived from inorganic processes producing methane in Earth's crust and mantle (Horita and Berndt 1999). Biogenic  $\text{CH}_4$  sources include both natural and anthropogenic ones, e.g. wetlands, rice paddies, ruminants, termites,

freshwater and marine sediments, and landfills (e.g. Quya et al. 1988, Prather 1995). Globally wetlands are the main natural source of CH<sub>4</sub> emissions to the atmosphere with recent estimates ranging from 177 to 284 Tg yr<sup>-1</sup> (IPCC 2013). According to Christensen et al. (2003a) one third to half of the emissions are from northern peat-forming wetlands (peatlands) and Gorham (1991) reported an annual release of 46 Tg yr<sup>-1</sup>.

## **1.2. Methane in northern peatlands**

### *1.2.1. Northern peatlands*

Peatlands can be roughly classified into bogs and fens depending on their water source and trophic status. Bogs are hydrologically isolated and have no connection to the groundwater. It is elevated from its surroundings and all of its water is derived from precipitation. Bogs are acidic and low-nutrient environments, and the vegetation is dominated by dwarf ericaceous shrubs and *Sphagnum* mosses. In an addition to rain, fens receive mineral-rich water from surface runoff and groundwater. Fens are less acidic and more nutrient-rich environments than bogs and the vegetation is characterized by sedges and bryophytes. (Laine and Vasander 1998)

Although northern peatlands in boreal and subarctic regions constitute less than 3% of Earth's terrestrial area (Rydin and Jeglum 2006) their waterlogged and anaerobic conditions make them significant sources of methane into the atmosphere. The northern peatlands have low decomposition rates due to low temperature, anoxic conditions, small microbial populations and high refractory content of plant litter (Moore and Basilisko 2006). They usually are sinks of carbon, removing CO<sub>2</sub> from the atmosphere via photosynthesis (Minkinen et al. 2002). Turunen et al. (2002) estimated the total carbon pool of boreal and sub-arctic peatlands at 270–370 Pg with an accumulation rate of 66 Tg yr<sup>-1</sup>. In Finland one third of the total land area is classified as mire but less than half of the mires are undrained (Alanen and Aapala 2015). Turunen et al. (2002) estimated the total carbon pool of Finnish undrained mires to be at 2257 Tg with a carbon accumulation rate of 0.79 Tg yr<sup>-1</sup>.

With the large amount of carbon stored and sizeable CH<sub>4</sub> emissions, the northern peatlands play an important role in carbon cycle (Gorham 1991) and could have significant implication to the further development of the greenhouse effect (Christensen et al. 2003a). By understanding the mechanics of peatland CH<sub>4</sub> production/consumption and the controls on CH<sub>4</sub> emissions, we can improve our predictions of future atmospheric greenhouse gas concentrations and the associated radiative forcing of the atmosphere (Christensen et al. 2003a).

### *1.2.2 Methane production, consumption and transport*

In peatland ecosystems methane cycling consists a number of biochemical processes. Bacterial CH<sub>4</sub> is the ultimate end-product of decomposition of organic matter by anaerobic microbial fermentation (Quya et al. 1988). Fermentative microbes, known as methanogens, a group of microorganisms solemnly belonging in to the domain Archaea, are capable of producing methane gas. Methanogens produce CH<sub>4</sub> as a metabolite in energy production, and metabolize only in anoxic conditions at redox levels Eh <- 300 mV (Kamal and Varma 2008). Methanogens generate CH<sub>4</sub> by several different pathways. In peatland ecosystems there are two main pathways for methanogenesis: acetate fermentation and CO<sub>2</sub>-reduction (Chanton et al. 2005). In acetate fermentation acetotrophic methanogens use acetate as a substrate to produce CH<sub>4</sub>:



In CO<sub>2</sub>-reduction hydrogenotrophic methanogens reduce CO<sub>2</sub> using H<sub>2</sub> as an electron donor:



Above reactions can be summarized to overall reaction that describes both pathways, as acetate can be written as 2CH<sub>2</sub>O:



In general, the more acidic bogs tend to favour methanogens that utilize  $\text{CO}_2$  reduction and less acidic fens, owing to higher supply of acetate exuding from the roots of vascular plants, tend to favour acetate fermentation (e.g. Horn et al. 2003, Galand et al. 2005, Hornibrook 2009). However, in some acidic environments, homoacetogenic bacteria are more efficient in scavenging  $\text{H}_2$  than methanogens, producing acetate (Whalen 2005). This leads the methanogenesis to proceed via acetotrophic methanogens. Predominant pathway also varies in different parts of vertical peat profile (Hornibrook et al. 1997). In general, upper layers of peat, with abundant supply of organic carbon, tend to favour acetate fermentation, and deeper peat layers are predominated by  $\text{CO}_2$  reduction.

The uppermost layer of peat tends to be an aerobic zone where some of the  $\text{CH}_4$  produced in the anaerobic zone is oxidized by methanotrophic bacteria (Whalen 2005). Methanotrophs are a group of bacteria that utilize methane as a sole source of carbon and energy (Hanson and Hanson 1996) and these reactions lead sequentially to methanol, formaldehyde, formate and finally carbon dioxide (Whalen 2005).

Methane is released to the atmosphere via three main pathways: diffusion, ebullition and plant-mediated transport (Lai 2009). Diffusive transport is the only pathway which facilitates the contact of  $\text{CH}_4$  with methanotrophs in the upper aerobic zone (Whalen 2005). About 20 to 40 % of  $\text{CH}_4$  produced in the anaerobic zone is oxidized during diffusion.

In ebullition,  $\text{CH}_4$  gas bubbles can escape, without the opportunity of oxidation owing to the low solubility of  $\text{CH}_4$  gas. Ebullitions are highly discontinuous and variable, both spatially and temporally (Whalen 2005). Through ebullition peatlands can emit a large amount of  $\text{CH}_4$  within hours and cover up to 50–64 % of total  $\text{CH}_4$  emitted from northern peatlands (Christensen et al. 2003b, Tokida et al. 2007).

In plant-mediated pathway aerenchymous vascular plants serve as ventilation systems, internally transporting  $\text{CH}_4$  from roots in the anaerobic zone to the peat surface, thus bypassing the methane-oxidizing, aerobic zone of peat (Whalen 2005). Vascular plants are more represented in sedge-dominated peatlands where most of the  $\text{CH}_4$  is released through plant-mediated pathway (Ding et al. 2004)



### *1.2.3 Methane emission controls*

Several independent studies have been made to understand the controls on CH<sub>4</sub> emissions in northern peatlands. Although emissions are highly variable, both spatially and temporally, controlling factors have been identified. They include soil temperature (Crill et al. 1993), water table position (Moore and Roulet 1993), net ecosystem production (NEP) of CO<sub>2</sub> (Whiting and Chanton 1993), and microbial substrate availability (e.g. Christensen et al. 2003a). Soil temperature has an effect on microbial CH<sub>4</sub> production and consumption rates. Water table level follows the microtopography, and determines the thickness of aerobic and anaerobic zones, and in general, a lower water table leads to smaller CH<sub>4</sub> fluxes (Lai 2009). Especially in wetter sites, NEP has been identified as good integrating variable, as it correlates with a number of controlling factors of CH<sub>4</sub> production, consumption and transport (Lai 2009). Also, the supply (Segers 1998) and the quality (Christensen et al. 2003a) of microbial substrate show strong correlation with CH<sub>4</sub> emission rates, with acetate being the most important of organic acids that methanotrophs use as substrates.

Explaining large scale variations in CH<sub>4</sub> emission is hard as northern peatlands demonstrate high variation among peatland types, microtopography, and consequently in rates of CH<sub>4</sub> fluxes. In general, individual studies find correlations up to few controlling factors as the controlling factors tend to override other possible factors (e.g. Christensen et al. 2003a, Bellisario et al. 1999, Whiting and Chanton 1993, Bubier et al. 1995).

### **1.3. Isotopic signatures as tools to understand methane production pathways**

Isotopic composition of methane can be used to trace the CH<sub>4</sub> formation pathway as each CH<sub>4</sub> source has its own characteristic <sup>13</sup>C/<sup>12</sup>C and D/H (Whiticar 1999). The most commonly measured isotopes of CH<sub>4</sub> sources are the stable isotopes <sup>13</sup>CH<sub>4</sub> and CH<sub>3</sub>D. The isotope data are denoted using the delta notation by δ<sup>13</sup>C and δD expressed here in permil (‰):

$$\delta_x = \left[ \frac{(R_a)_{sample}}{(R_a)_{standard}} - 1 \right] 1000 (\text{‰}), \quad (\text{Eq. 4})$$

where  $R_a$  is the  $^{13}\text{C}/^{12}\text{C}$  or D/H ratios relative to standards which are Vienna Peedee Belemnite (VPDB) for  $^{13}\text{C}/^{12}\text{C}$  and Vienna Standard Mean Ocean Water (VSMOW) for D/H.

The isotopic composition of atmospheric methane ( $\delta^{13}\text{C}_{\text{CH}_4}$ ) depends on the proportion of  $\text{CH}_4$  input from different sources. The global average of  $\delta^{13}\text{C}_{\text{CH}_4}$  in Northern Hemisphere is  $-47.4 \text{ ‰}$  (Stevens and Walen 2000). Abiogenic methane has mean  $\delta^{13}\text{C}$  values significantly higher than those of biogenic  $\text{CH}_4$  (Quya et al. 1988). Bacterial  $\text{CH}_4$  has  $\delta^{13}\text{C}$  values varying from  $-110 \text{ ‰}$  to  $-50 \text{ ‰}$  (relative to VPDB) and  $\delta\text{D}$  from  $-400 \text{ ‰}$  to  $-150 \text{ ‰}$  (relative to VSMOW) (Whiticar 1999). Knowing the isotopic composition of  $\text{CH}_4$  sources is needed, when the global budget for  $\text{CH}_4$  sources and sinks is developed.

In peatland ecosystems processes,  $\text{CH}_4$  production and consumption are subjected to kinetic isotope fractionation, as methanogens and methanotrophs both utilize lighter molecules more frequently than the isotopically heavier species (Whiticar 1999). In general, methane produced via acetoclastic pathway is less depleted in  $^{13}\text{C}$  than methane produced via  $\text{CO}_2$  reduction. Lasting assumption has been that acetoclastic methanogenesis dominates in freshwater systems (Whiticar et al. 1986, Whiticar 1999), because higher plant productivity ensures a more abundant supply of fresh organic material, but less productive sites can be dominated by  $\text{CO}_2$  reduction (e.g. Lansdown 1992). The reported  $\delta^{13}\text{C}$  for wetland  $\text{CH}_4$  ranges approximately between  $-100 \text{ ‰}$  (Chanton et al. 2002) and  $-42 \text{ ‰}$  (Gerard and Chanton 1993). Still a single collective  $\delta^{13}\text{C}_{\text{CH}_4}$  value of  $-60 \text{ ‰}$  is usually given when applied to wetland  $\text{CH}_4$  budgets constrained by stable isotopes (Hornibrook 2009). The wide range of the  $\delta^{13}\text{C}$  in produced methane is a demonstration of the complexity in the processes governing the production, as the source of that produced  $\text{CH}_4$  is almost solemnly C3 type vegetation that exhibits carbon isotope compositions in a narrow scale from  $-20$  to  $-37 \text{ ‰}$  (Kohn 2010).

#### 1.4. Aims of the study and the main hypothesis

For this study, CH<sub>4</sub> gas samples were collected from both ombrotrophic and minerotrophic sites of the Siikaneva mire complex in order to find out the isotopic composition and to calculate the CH<sub>4</sub> flux of methane emitted from different types of sampling plots, representing variation in microtopography. In addition to the gas samples, pore water samples were collected adjacent to the sampled plots, from the depth of 50 cm, in order to identify differences in isotopic composition of dissolved inorganic carbon (DIC) in relation of microtopography. In addition, as a part of this thesis, a standard operating procedure was created for the instrument used to analyse the isotope samples in order to produce as reliable and accurate data as possible.

The Siikaneva mire was selected as the measurement site, because plenty of ecological and geological information is available for the site. Other studies from the measurement sites, with relevance to this thesis, are of carbon exchange (e.g. Aurela et al. 2007, Riutta et al. 2007, Uljas 2015) and CH<sub>4</sub> flux (e.g. Rinne et al. 2007, Riutta et al. 2007).

The overall aim of my study is to learn how microtopography effects CH<sub>4</sub> emission and its  $\delta^{13}\text{C}$  values at the Siikaneva bog and fen. Results may also reveal information about the controlling factors of CH<sub>4</sub> emissions and provide evidence for methane production pathways. Though there have been many studies related to  $\delta^{13}\text{C}_{\text{CH}_4}$  in peatlands, and even a greater number about CH<sub>4</sub> emissions from peatlands, the processes contributing to them are complex and interacting with each other. As high variations exists both within and between peatland ecosystems, more studies are needed in order to produce large scale principles of peatlands contribution to global carbon cycle and greenhouse gas budget.

The hypothesis of my study is that microtopography on both sites is an integrating controlling factor of CH<sub>4</sub> emissions, and that isotopic composition of the emitted CH<sub>4</sub> would reflect the processes beneath the peat surface resulting in variations in the  $\delta^{13}\text{C}$  values between sampled plots. Though this study handles both sites quite individually, since the difference between the sites from a biological perspective is obvious, the hypothesis is that there should be less acetate fermentation on the bog than on the fen, and this should be also evident in the isotope data. Hence, it is expected that at the

minerotrophic site the isotopic values reflect more nutrient-rich environment and that at the ombrotrophic site the isotopic values of CH<sub>4</sub> are more depleted in <sup>13</sup>C.

## **2. STUDY AREA**

The Siikaneva mire reserve is the largest boreal mire complex in Pirkanmaa, Southern Finland (Fig. 1), at the border of the southern and middle boreal vegetation zones (Ahti et al. 1968). Its total surface area is approximately 1560 ha from which the peat covers up to 1215 ha (Silvan et al. 2008). Siikaneva is a large natural mire compared to a typical Finnish south boreal mire setting, as only the fifth of the original peatlands in south boreal Finland are undrained and less than 2 % of these peatlands are protected under mire conservation program (Alanen and Aapala 2015).

### **2.1. Geological setting**

The northern side of Siikaneva borders on the Näsijärvi-Jyväsylä end moraine. From northeast and northwest sides it borders on the delta formations of Siikakangas and Särkikangas, and from the southern side it borders on moraine and bedrock hills of the Siikajärvi lake upland. (Silvan et al. 2008)

The Siikaneva mire complex consists of several different mire types but can be divided into two main types based on hydrogeology, topography and substrate availability; the ombrotrophic bog and the minerotrophic fen (Silvan et al. 2008). The ombrotrophic parts of Siikaneva are mainly concentrated to the northern side of the mire where they partly overlay the flat delta formations. The minerotrophic aapa mires are mainly located at the south/southeast side of Siikaneva where more nutrient rich waters inflow from the lake upland and young boreal forests. (Silvan et al. 2008)

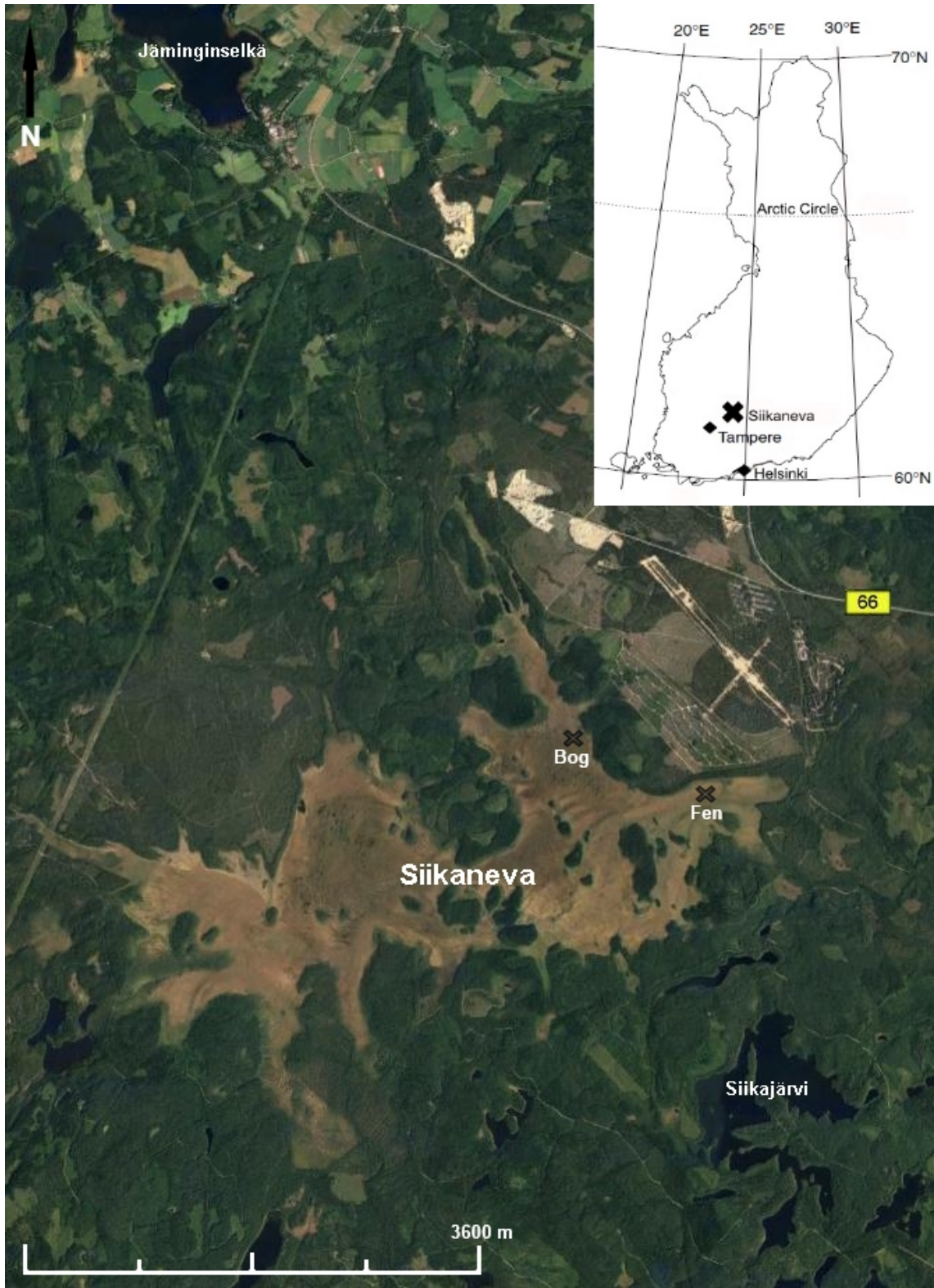


Figure 1. Upper corner: Location of Siikaneva, Pirkanmaa, Finland, redrawn from Rinne et al. (2007). Large picture: An aerial view of Siikaneva and its surroundings, depicting both measurement sites. Image modified from Google Earth still.

Siikaneva has eight outflows to the surrounding water systems. The main outflows are Rooppioja to the south and Jouttipuro to the east, which both flow through Lake Orivesi and end up to Lake Längelmävesi. From the west side Siikaneva drains to Lake Näsijärvi and from the north side it drains to Lake Jäminginselkä. All the waters of Siikaneva flow through the River Kokemäenjoki to the Bothnian Sea. (Silvan et al. 2008)

Parts of the Siikaneva mire started to accumulate peat already in the preboreal age in the early Holocene, right after the ice masses retreated. No deep water marine sediments have been found underneath the peat layers which indicate that the Yoldia Sea was quite shallow at the location. The sediments under the peat are silts and sands from the deltas and in some areas the peat borders on bedrock. Through the evolution of wetlands, the primarily formed minerotrophic fens dominated by *Carex* have since depleted from nutrients and peat layers have risen above the effects of runoff and groundwater. This process known as ombrotrophication, i.e. the development from fen to bog (Korhola and Tolonen 1998), is the main reason why 70 % of the peat layers in Siikaneva are dominated by *Sphagnum* mosses. (Silvan et al. 2008)

The average peat depth in Siikaneva is 2.6 m. On the eastern side of the mire the average peat depth is around three meters and quite large areas reach into the depth of around five meters. On the areas where the mire sits on top of the delta formations the peat depth is relatively low. The total volume of peat deposits at Siikaneva is around 32 M m<sup>3</sup>, and the peat accumulation rate has been on average 0.9 mm yr<sup>-1</sup>. (Silvan et al. 2008)

## 2.2. The study sites

Both measurement sites of this study, as seen in Figure 1, are located at the eastern side of the mire complex. On the ombrotrophic bog (61°50'N, 24°10'E, 167 m a.s.l.) the vegetation is dominated by *Sphagnum* mosses (e.g. *Sphagnum majus*, *S. rubellum*, *S. cuspidatum*) and dwarf shrubs (e.g. *Calluna vulgaris*, *Empetrum nigrum*, *Vaccinium uliginosum*) (Uljas 2015). Almost a third of the peat area is either muddy or under water, though during the growing period the open water areas shrink significantly.

The microtopography of the bog is more pronounced than that of the fen. Especially the hummocks are clearly elevated from the surroundings. The average pH of the bog is 4.1 (unpubl.data of Korrensalo 2012).

The minerotrophic site (61°50'N, 24°11'E, 162 m a.s.l.) is an oligotrophic (poor) fen, and the peat depth is up to four meters (Rinne et al. 2007). Its dominating vegetation consists of *Sphagnum* mosses (e.g. *Sphagnum balticum*, *S. majus*, *S. papillosum*), Sedges (*Carex rostrate*, *C. limosa*, *Eriophorum vaginatum*) and pod grass (*Scheuchzeria palustris*). The microtopography is relatively flat with no distinct hollow and sting structures. The fen is not noticeably less acidic than the bog with average pH of 4.2 (Aurela et al. 2009).

### **2.3. Weather conditions**

The closest weather station to Siikaneva is at Hyytiälä, located 5 kilometers from the mire. During 1981-2010, the annual mean temperature was 3.5°C, and the annual precipitation was 711 mm (Pirinen et al., 2012). During the growing period (May to August) in 2015 the monthly mean temperatures were very close to the decadal monthly mean temperatures ranging from 8.4°C to 15.2°C, as seen in Figure 2. The growing period precipitation rates (Fig. 3) also neared the decadal mean values, except in August (precipitation 12.6 mm) which was much drier than the 30-year average (precipitation 85 mm). Almost all field days were cloudy and rainy, and the conditions prevented the chamber temperatures from rising distinctly above the measured air temperatures.

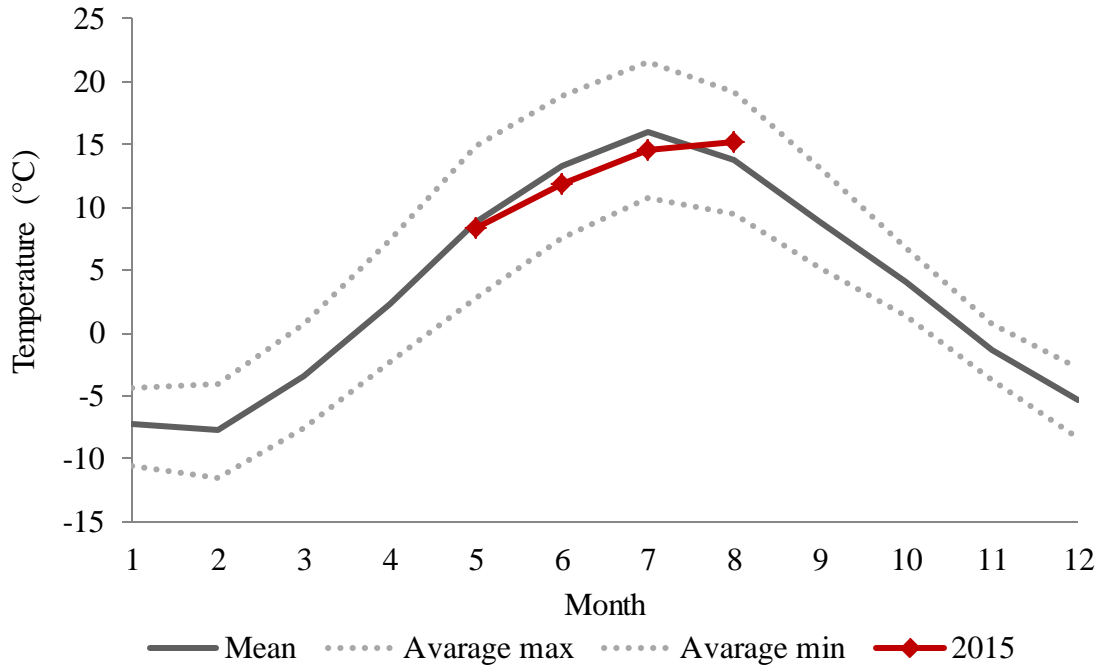


Figure 2. Mean monthly temperatures and means of daily maxima and minima during 1981-2010, and monthly mean temperatures during measurement months at the Hyttiälä weather station. The statistics from 1981 to 2010 are from Pirinen et al. (2012), and the values from 2015 are from Finnish Meteorological Institute's Open Data datasets.

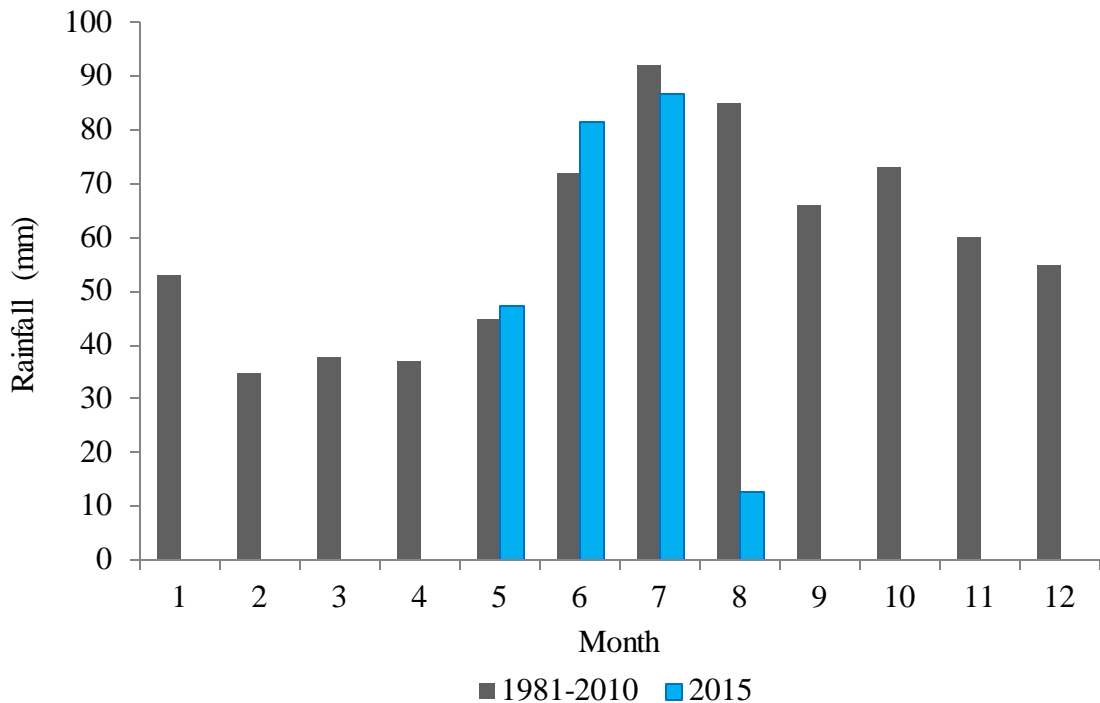


Figure 3. Mean monthly precipitation during 1981-2010 and during the measurement months at the Hyttiälä weather station. The statistics from 1981 to 2010 are from Pirinen et al. (2012), and the values from 2015 are from Finnish Meteorological Institute's Open Data datasets.



### 3. MATERIALS

Daytime samples for this study were collected once a month from May to August in 2015, at the end of each month. Both measurement sites, the bog and the fen, had pre-existing collars installed to the representative plots. The surface of a boreal peatland can be divided into microscale subunits, microsites, according to water table levels and main vegetation communities (Becker et al. 2008).

To this study, three microsites were selected from both of the sites, representing the most pronounced microtopographical variation at the sites. At the bog they were hollow (HO), high lawn (HL) and high hummock (HHU), and at the fen they were hollow (HO), *Carex* lawn (CR) and hummock (HU). Hummocks are elevated from their surroundings and their average water table is over 20 cm below the peat surface (Saarnio et al. 1997). Lawns are intermediately wet with water table ranging from 5 to 20 cm below the peat surface, and hollows are the wettest with water table level up to 5 cm below the peat surface.

In May, June and July, three different plots per microsite (set of plots) were used for repetitive samples. In August, all repetitive gas samples were taken from the same set of plots to enhance the reliability of the isotope samples. In August, also nighttime measurements for gas samples were conducted, as it represented the largest diurnal variation in solar radiation and air temperature. Same plots were used than those in the daytime measurements, but repetitive samples were not collected, as both sites were sampled during the same night.

#### 3.1. Methane concentration samples

The concentration samples of CH<sub>4</sub> were gathered with closed chamber method (e.g. Moore and Knowles. 1990, Nykänen et al. 1998, Riutta et al. 2007). Opaque aluminium chambers (60 x 60 x 30 cm) were placed on top of the collars that reached 20–30 cm below the peat surface (Fig. 4). Chambers were sealed from air leaks by adding water to the grooves in the collars, and at the start of each measurement a rubber

plug equipped with a tube and a sensor was placed on the hole on top of the chamber. Chambers were also equipped with battery operated fans to mix the air inside. To measure the changes in the CH<sub>4</sub> concentration within the chambers, gas samples were withdrawn using tubes attached to 60 mL plastic syringes with a three way stopcock kept open during the measuring period. The samples were drawn at 5, 15, 25 and 35 min from the enclosure. In June, the measuring period was extended, and a fifth sample was drawn at 60 min from the enclosure. This was done to ensure a sufficiently high methane concentration for isotope analyses. For each collection, syringes were flushed with chamber air before drawing the sample. Collected samples were injected with excess pressure into 10 mL vacuumed septum sealed glass vials and stored upside down in refrigerator temperatures. A total of 336 samples were collected, and all the plots per site were sampled during the same day every month, except in May when bog samples were collected on consecutive days.

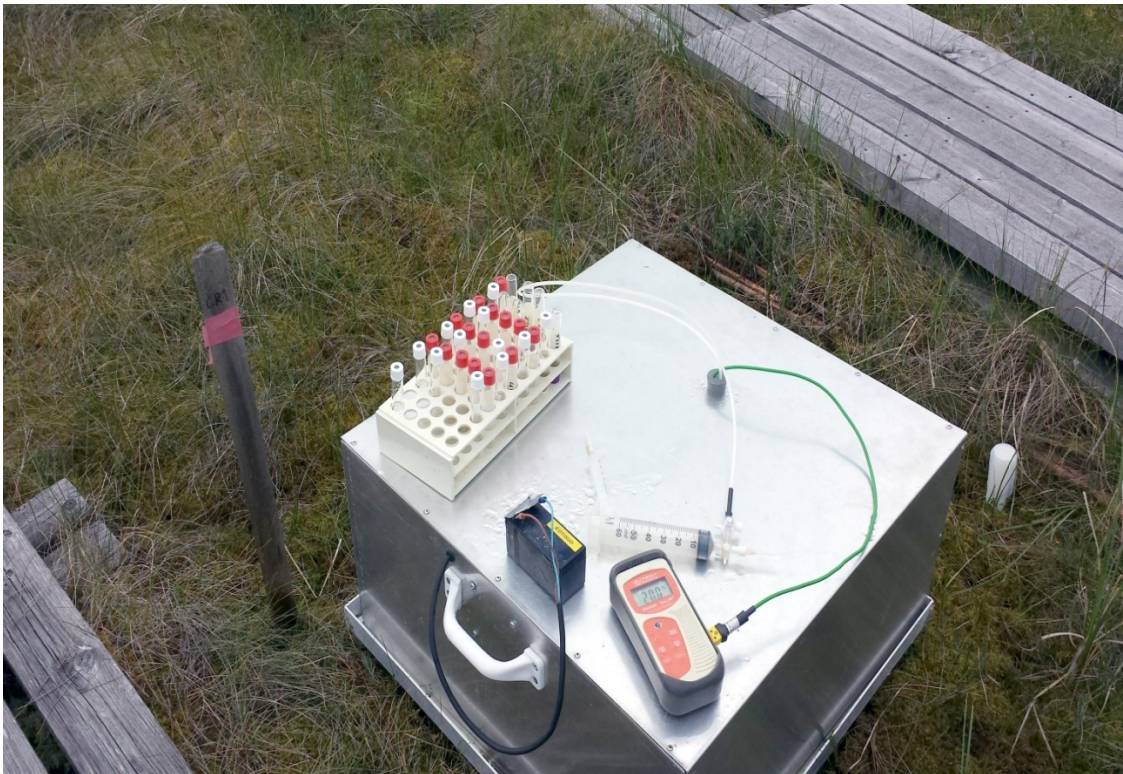


Figure 4. Closed chamber measurement in June, with the required equipment. The plot is *Carex* lawn (CR1) on the fen. Right next to the chamber is the pipe used to access pore water.

### 3.2. Methane isotope samples

Samples of emitted methane for the isotope analysis were collected at the same time and in same manner as the CH<sub>4</sub> concentration samples. Septum sealed glass vials used were either helium flushed or had vacuum inside. In May, the samples were collected at 25 and 35 min from the enclosure to 10 mL vials. In June, samples were collected at 35 and 60 min from the enclosure. In July, samples were collected into 100 mL septum sealed vials, which is the size required to measure CH<sub>4</sub> at atmospheric concentrations. These samples were collected at 5 min and 35 min from the enclosure. In August, isotope samples were collected in the same way at 5 and 35 min from the enclosure. To fill up 100 mL vials, two 60 mL syringes were joined side by side with three way stopcocks. Collected samples were stored in refrigerator temperatures before analysis. A total of 156 samples were collected.

### 3.3. DIC samples

Pore water samples for DIC analysis were collected from plastic pipes adjacent to the chambers in May, July and August. The pipes had nylon socks as pre-filters and holes drilled to the collection depth. Samples were withdrawn from a depth of 50 cm with a plastic tube attached to a 10 mL syringe. The tube had an extra nylon sock filter that was changed at each different collection site. The pipes were emptied from stagnant water before samples were withdrawn. The samples were filtered through Acrodisc 0.8/0.2 µm syringe filters and injected to helium flushed, pre-acidified vials that were stored in refrigerator temperatures before analysis.

Due to a high concentration of organic matter, field filtering proved to be a challenge. For this reason, repetitive samples were not collected from each set of plots. In May, two samples were collected from each plot on one set of plots (n = 6). In July one sample was collected from each plot (n = 9), and in August three samples were collected from two sets of plots (n = 18/15). In August, at the fen, two of the pipes at hummocks were dry, and so the samples were drawn only from one pipe.

### 3.4. Other measurements

Air temperatures were measured from inside and outside of the chambers, and peat temperatures were measured at depths of 5, 15 and 30 cm, using the Eutech Instruments EcoScan Temp JKT. Water table levels were measured close to the chamber locations. Unlike the chamber measurements, the water table levels were measured from three different plots per microsite each month, except on the fen, where in August the pipes used to measure water table levels were dry at the two of the three hummock plots.

Initially, it was also intended to analyse  $\delta^{13}\text{C}_{\text{CH}_4}$  from the pore water samples collected in the same manner as the  $\delta^{13}\text{C}_{\text{CO}_2}$  from the DIC samples. Unfortunately,  $\delta^{13}\text{C}_{\text{CH}_4}$  pore water samples were too small to be analysed.

## 4. METHODS

### 4.1. Methane concentration and flux

#### 4.1.1. Physical methods

$\text{CH}_4$  concentration samples from closed chamber measurements were analysed with gas chromatograph equipped with flame ionization detectors at Hyytiälä forest station in the autumn of 2015. The used instrument was an Agilent Gas Chromatograph (model 7890A, Agilent Technologies, USA).

#### 4.1.2 $\text{CH}_4$ flux calculations

$\text{CH}_4$  flux for each plot was calculated from the mass balance of  $\text{CH}_4$  in the chamber air and a linear regression of the chamber concentration change with time (e.g. Christensen et al. 2003a). Used equation was:

$$F_{CH_4} = \frac{dC}{dt} * h, \quad (\text{Eq. 5})$$

where  $F_{CH_4}$  is the flux of  $CH_4$  ( $mg\ m^{-2}h^{-1}$ ),  $C$  is the  $CH_4$  concentration in the chamber ( $mg\ m^{-3}$ ),  $t$  is time (h) and  $h$  is the height of the chamber (m) (Pihlatie 2007). At least three samples per measurement were used to create the linear regression, and all measurements with coefficient of determination ( $R^2$ ) < 0.8 were left out as poor quality data (Christensen et al. 2003a).

Pearson correlation and least-squares regression analyses were applied to find relationships between fluxes and measured environmental parameters (water table and peat temperature).

#### **4.2. Stable isotope analysis of methane**

The  $\delta^{13}C_{CH_4}$  samples were analysed at the Department of Geosciences and Geography of the University of Helsinki using a gas chromatography-based continuous-flow isotope-ratio mass spectrometry (IRMS). The instrument was a Thermo Scientific Delta Advantage mass spectrometer complemented by a Gas Bench II and a PreCon, automated trace gas pre-concentrator. According to the manufacturer, the external precision for  $\delta^{13}C_{CH_4}$  results in natural concentration (1.7 ppm / 100 mL) is 0.5 ‰ (PreCon operating manual).

The PreCon had been unused for some time and standard operating procedures for it were not available. As the PreCon was restored to working order (by a professional) at the end of the summer 2015, all the  $\delta^{13}C_{CH_4}$  samples were collected before we had a verification that the PreCon worked reliably. Hence, alterations to measurement procedures (chamber enclosure length and vial size) during the growing period were based on estimates.

#### 4.2.1. Setting up the PreCon

Figure 5 shows the schematic of PreCon. Unlike depicted in the figure, the actual samples were operated manually with a two line needle injected into a septum sealed vials for continuous sample transfer. The sample containers with manual valves were used in a few test runs to see if there was a systematic difference between the two types of sample containers.

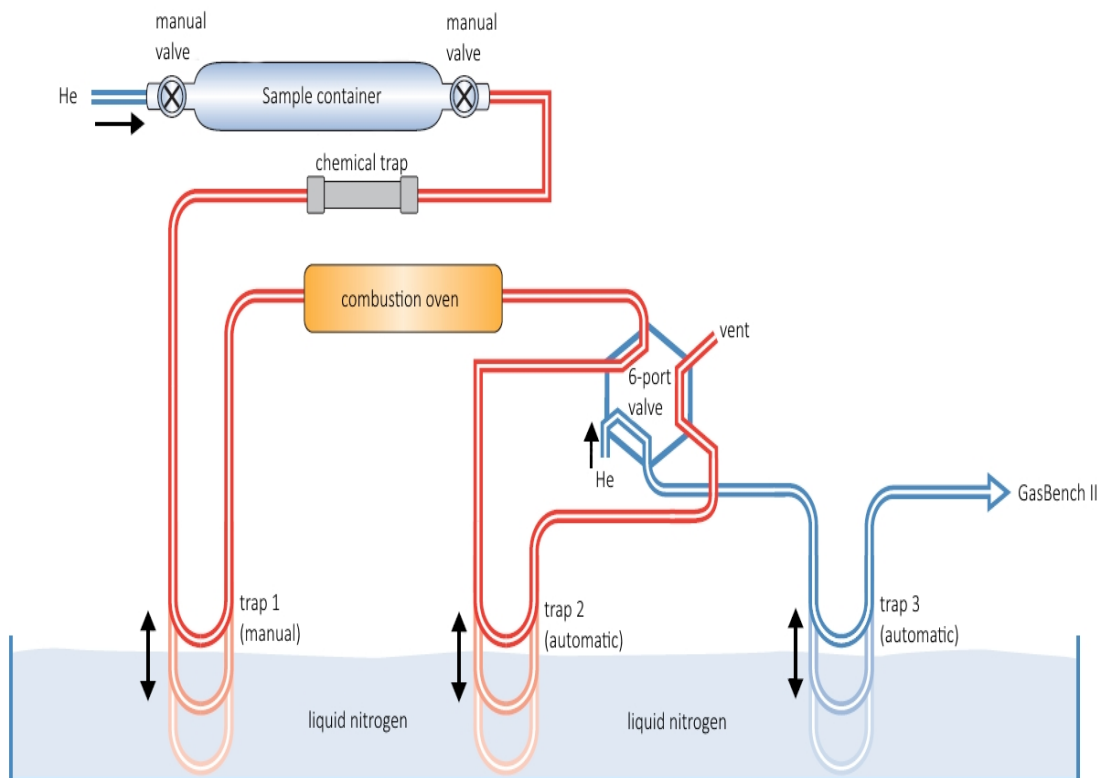


Figure 5. Schematic of PreCon (modified from PreCon operating manual). The sample is carried in helium flow from the sample container. The ascarite chemical trap withholds water and captures approximately 99.99 % of the gas samples  $\text{CO}_2$ . Trap 1 operates manually and is kept down in the liquid nitrogen the whole time analyses are made. It captures all  $\text{CO}_2$  that escaped the chemical trap. The combustion oven ( $1000\text{--}1100^\circ\text{C}$ ) oxidizes  $\text{CH}_4$  to  $\text{CO}_2$  and  $\text{H}_2\text{O}$  with 100 % combustion efficiency. Trap 2 is automatic and the freeze time can be adjusted from user interface. It freezes all the combusted  $\text{CO}_2$  derived from  $\text{CH}_4$  and forms a sampling loop with the 6-port Valco valve. The Valco valve switches from the load position to the inject position. Trap 3 is also automatic and serves as cryofocuser before the sample is transferred to GasBench II which is calibrated to analyse  $^{13}\text{C}/^{12}\text{C}$  ratios.

For the test runs, air samples were collected from the lab air. A total of 69 samples were analysed in the tests. The first half of the tests were made with individual air samples collected just prior to the analysis, as the air in the lab gave indicative results to adjust major parameters. The aim was to establish the optimal parameters for the analysis, mainly adjusting the CO<sub>2</sub> reference gas for linearity, and tweaking the sample collection length from the container, to achieve non-fractioning sample collection. It was also confirmed that the repetitive samples gave  $\delta^{13}\text{C}_{\text{CH}_4}$  results within the reported precision.

The reproducibility of the analyses was tested by leaving a group of 100 mL vials open for the night so the air inside them balanced with the air in the lab. The vials were then closed simultaneously and analysed. A few samples were purposely stored for longer periods to test for possible leakages from the containers. The groups yielded  $\delta^{13}\text{C}_{\text{CH}_4}$  values of  $-45.9 \pm 0.2$  for Group 1,  $-46.5 \pm 0.2$  for Group 2 and  $-39.0 \pm 0.3$  for Group 3 (Fig. 6). The reproducibility of the analyses is within the limits indicated for the instrument. The sample collection time for 100 mL vials was set to 800 s, which resulted good linearity and non-fractioning sample collection. Collection times under 700 s resulted bad linearity and failed to yield repetitive isotope results. For 10 mL vials, test runs with atmospheric concentrations of CH<sub>4</sub> were not reliable due to inadequate sample size. The sample collection time for field samples in a 10 mL volume was estimated and set to 500 s to ensure non-fractioning sample collection.

As a part of the operation practice, each analysis session was started with an individually collected air sample, as the early tests indicated low linearity result for the first analysis of the day. Even though there was a constant flow of helium in the PreCon system, this wake-up run ensured more reliable results, since it helped to cleanse the system from any unwanted particles.

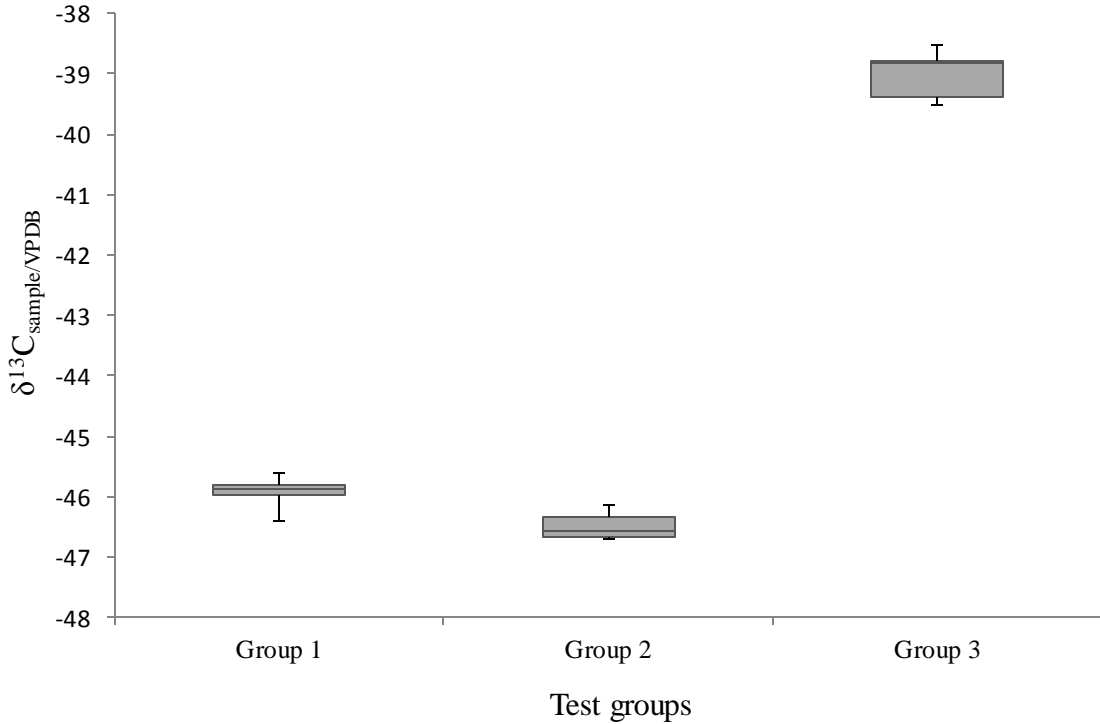


Figure 6. Box plot of  $\delta^{13}\text{C}_{\text{CH}_4}$  results for three separate groups of air samples showing minimum, maximum and median. These groups were analysed after establishing adequate sample collection time of 800 s for the 100 mL vials. Group 1 ( $n = 7$ ) and group 2 ( $n = 6$ ) showed similar  $\delta^{13}\text{C}$  values (approx. -46 ‰) than individually collected samples. Two of the samples in group 2 were analysed after a month of storing. Group 3 ( $n = 7$ ) gave unexpected but uniform results. The possible source for the  $^{13}\text{C}$ -enriched values could only be guessed, as after few days the measured  $\delta^{13}\text{C}$  values from the lab air were yet again close to the global atmospheric mean value.

#### 4.2.2 Isotopic analysis of field samples

The Siikaneva samples were analysed using the operation procedures developed during the test runs. Since the laboratory lacked an industrially produced quality standard to verify the accuracy of the results, simultaneously collected batches of lab air were used to monitor reproducibility. Limited by the number of 100 mL vials, three separate groups of air samples were used as quality standards (Fig. 7). The groups yielded  $\delta^{13}\text{C}_{\text{CH}_4}$  values of  $-45.1 \pm 0.2$  for Group 1,  $-45.1 \pm 0.3$  for Group 2 and  $-43.0 \pm 0.1$  for Group 3. The variation of the  $\delta^{13}\text{C}_{\text{CH}_4}$  values in the individual groups of the quality standards remained within the reported precision.



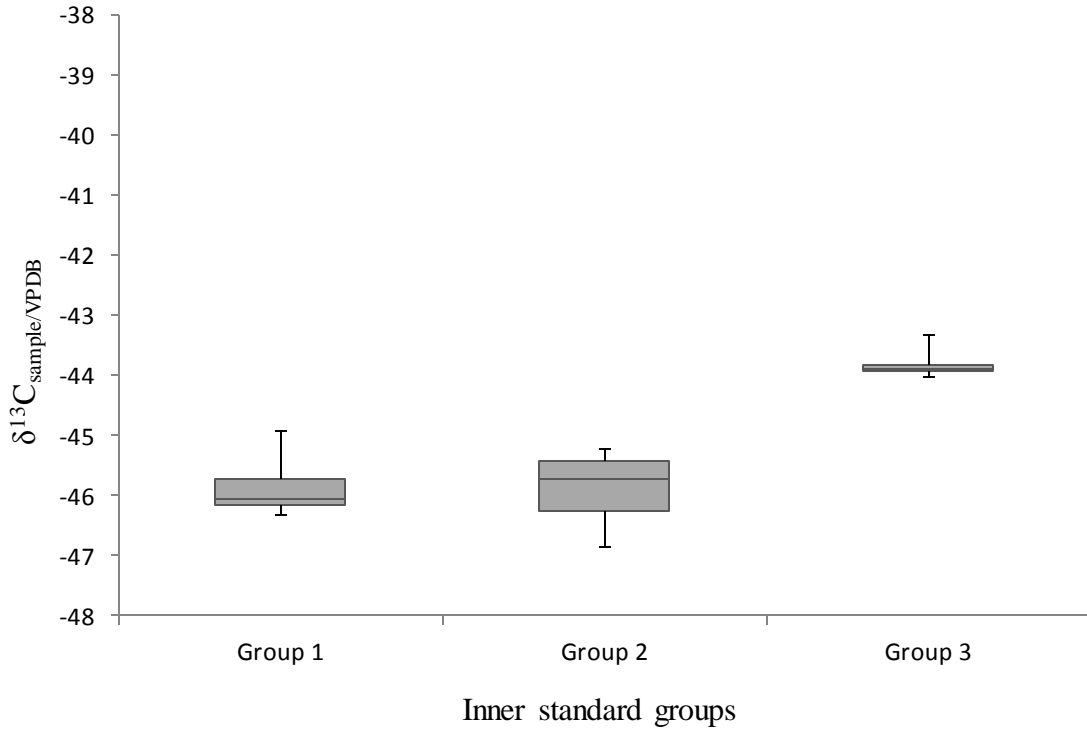


Figure 7. Box plot of  $\delta^{13}\text{C}_{\text{CH}_4}$  results showing minimum, maximum and median for the three groups of air samples used as a quality standard in the Siikaneva sample analysis. For each group  $n = 15$ .

The initial results from the mass spectrometer are given relative to the  $\text{CO}_2$  gas used as a reference. Since our LIMS (Laboratory information management system) was not programmed with the required information to report  $\text{CH}_4$  results relative to VPDB, the conversion from the  $\text{CO}_2$  standard to VPDB was done manually. The isotopic composition of tank  $\text{CO}_2$  was calculated from previous measurements of a laboratory carbonate standard with a  $\delta^{13}\text{C}$  value of 0.404 ‰ using Equation 6.

$$\delta_{\text{CO}_2/\text{VPDB}} = \left( \frac{\delta_{\text{std}/\text{VPDB}} - \delta_{\text{std}/\text{CO}_2}}{\delta_{\text{std}/\text{CO}_2} + 1000} \right) * 10^3 \quad (\text{Eq. 6})$$

The  $\delta^{13}\text{C}$  value of the sample was then calculated from Equation 7.

$$\delta_{\text{sample}/\text{VPDB}} = \delta_{\text{sample}/\text{CO}_2} + \delta_{\text{CO}_2/\text{VPDB}} + \left( \frac{\delta_{\text{sample}/\text{CO}_2} * \delta_{\text{CO}_2/\text{VPDB}}}{10^3} \right) \quad (\text{Eq. 7})$$

Since the CH<sub>4</sub> concentration varied significantly (from 2 ppm to 74 ppm), adjustments to the flow rate of the CO<sub>2</sub> reference gas were made prior to every sample analysis. Partial samples were also drawn from samples with higher CH<sub>4</sub> concentration in order to stay in range of an acceptable linearity. Results with bad linearity were discarded. All adjustments were estimated based on CH<sub>4</sub> concentration data that was analysed prior to the isotope samples.

#### 4.2.2 Methane isotope data analysis

The Keeling plot method (e.g. Keeling 1961, Pataki et al. 2003, Sriskantharajah et al. 2012) was used to identify  $\delta^{13}\text{C}_{\text{CH}_4}$  source signatures at sites and microsites, by plotting  $\delta^{13}\text{C}$  vs. the inverse of the CH<sub>4</sub> concentration. The CH<sub>4</sub> concentration at the site reflects the combination of background atmospheric CH<sub>4</sub> and gas added by the sources, and as the basis of Keeling plot method is the conservation of mass, the following equations can be derived (Pataki et al. 2003):

$$c_a = c_b + c_s \quad (\text{Eq. 8})$$

$$\delta^{13}\text{C}_a c_a = \delta^{13}\text{C}_b c_b + \delta^{13}\text{C}_s c_s, \quad (\text{Eq. 9})$$

where  $c_a$  is the CH<sub>4</sub> concentration measured in the chamber,  $c_b$  the background CH<sub>4</sub> concentration and  $c_s$  CH<sub>4</sub> concentration added by the source; and  $\delta^{13}\text{C}$  represents the carbon isotope ratio of each CH<sub>4</sub> component. Equation 9 can be expressed in linear form  $y = m/x + b$ :

$$\delta^{13}\text{C}_a = c_b (\delta^{13}\text{C}_b - \delta^{13}\text{C}_s) * \left(\frac{1}{c_a}\right) + \delta^{13}\text{C}_s, \quad (\text{Eq. 10})$$

where the y-intercept is the value of the source signature.

Standard linear regression (least-squares regression or Model I regression) assumes that that  $y$  (here the measured  $\delta^{13}\text{C}$ ) is dependent on  $x$  (here the inverse of CH<sub>4</sub> concentration) and  $x$  is independent and has no errors associated with it. Hence, reduced major axis regression (a.k.a. standard major axis regression, geometric mean regression or Model II regression) was applied to the constructed keeling plots, as it assumes that

both  $x$  and  $y$  are measured, and both include some error. In the reduced major axis regression, the slope of the regression line is the geometric mean of the least-squares regression line of  $y$  on  $x$  and the least-squares regression line of  $x$  on  $y$  (e.g. Sokal and Rohlf 1995). Pearson's correlation coefficient ( $R^2$ ) was applied to assess the goodness of the fit.

### 4.3. DIC analysis

Pore water  $\delta^{13}\text{C}_{\text{DIC}}$  samples were analysed from vial head-space using the same isotope ratio mass spectrometer (Thermo Scientific Delta Advantage, equipped with Gasbench II) as that used for the  $\delta^{13}\text{C}_{\text{CH}_4}$  samples. Analysed together with quality and calibration standards, the results are presented relative to VPDB. No additional statistical methods were used to process the DIC data.

### 4.4. Sources of error and uncertainty

#### 4.4.1. Sampling and storing samples

Much care was taken to minimize errors in field sampling in order to produce accurate data. Vials and collectors were visibly air tight, minimizing their vulnerability to leaks that would contaminate or fractionate the samples. The reagents of DIC analysis, in addition to other vials and collectors, were all of the required purity level.

The storing of isotope samples stretched over intended time span and samples collected in May were analysed after seven months from collection. Nevertheless, the isotope results were coherent with the  $\text{CH}_4$  flux data, and to add to their reliability, the overpressure injected to the 10 mL vials in sampling was still present in the analysis phase. The 100 mL vials were never filled with overpressure, but demonstrated the same coherency in results than the smaller vials.

For the peat temperature measurements, the thermometer in use malfunctioned in July and some the peat temperatures from both sites were not measured during the chamber

measurement at the designated plots, but the temperatures were measured within a 24 hour time frame. However, this only should have affected the peat temperatures at the depth of 5 cm since the temperatures at deeper layers are not so susceptible to short term variation, and the weather conditions were very similar on consecutive days.

#### *4.4.2. Chamber measurements*

Although closed chamber method is widely used in gas flux and isotope measurements, it has several limitations. Chamber closure can lead to disturbances in the microenvironment inside the chamber, by changing air pressure, temperature and diffusion gradient which biases the measured flux compared to ambient conditions (Davidson et al. 2002). Also, the collars used to seal the chambers from air leaks disturb the plant communities, as they reach to the root zone, and affect the hydrological flow in the upper peat layer.

Because the spatial variation in CH<sub>4</sub> emissions is great at the microsite level, extrapolating the flux data and the related isotope data to the ecosystem level is hard. This is especially relevant in this study, as the repetitive August chamber measurements were conducted at the same set of plots. The inner variability in the August measurements (Table 1 and 3) highlights these transient changes in flux rates that occur in the scale of hours. These sudden changes in emissions cannot be measured using the closed chamber technique conducted with monthly intervals.

#### *4.4.3. Isotope analysis and the Keeling plot method*

Analytical results between samples collected in helium flushed vials showed no visible difference to those collected in vacuumed vials. This was evidenced when creating partial samples from field samples that were presumed to contain too high CH<sub>4</sub> concentration to direct analysis. The partial samples were all injected to helium flushed vials whereas field samples were contained in both types of vials. Variation in analysis results, from the repetitive partial samples, derived only from change in linearity. However, using partial samples might have resulted in small fractionation effect, since the partial samples were collected using needles and syringes. Hence, the results of these partial samples could be slightly more negative than the actual field samples, because

lighter isotopes move more quickly. It is not clear whether this fractioning effect is within the precision of the PreCon, as the materials were not sufficient enough to perform such a thorough testing.

At both sites, using true background values for the atmospheric CH<sub>4</sub> concentration and isotope composition instead of global means, would likely have resulted in even higher correlation coefficient values in the Keeling plots. Using the background values (CH<sub>4</sub> concentration = 2.06 ppm and  $\delta^{13}\text{C}_{\text{CH}_4} = -44.93 \text{ ‰}$ ) of another south boreal Finnish natural mire (unpubl.data of I. Forbrich and N.Welti from Dorodnikov et al. 2013), the background values plot much closer to the regression line.

Ideally, Model II regression (in this case the geometric mean regression) should be applied to data sets containing over 60 samples, as the confidence intervals are large when data sets are small (Legendre 2013). However, applying Model I regression to the data set results in up to 3 ‰ less negative intercept values with much lower correlation, and thus does not produce as good fit. Pataki et al. (2003) reported a similar bias in the intercept values between the two regression methods.

## 5. RESULTS

### 5.1. Methane flux results

#### 5.1.1. Bog

Throughout the growing period, all samples had positive CH<sub>4</sub> flux values. The mean of the emissions was the highest on hollows (136–151 mg m<sup>-2</sup>d<sup>-1</sup>) and the lowest on hummocks (53–93 mg m<sup>-2</sup>d<sup>-1</sup>). The results of the CH<sub>4</sub> flux measurements are in Table 1 represented by two values; the first values are the results from May to July, and the values in parenthesis are the results from May to August, also including the non-repetitive night measurements. Since all the three repetitive daytime measurements in August were sampled from one set of microsites, the results do not represent the

microsite types comprehensively and thus are reported separately. The total emission for the growing period at the measured plots was 108–113 mg m<sup>-2</sup>d<sup>-1</sup>.

In May, June and July, the emissions rates decreased in the order hollow > high lawn > high hummock (Table 2 /Appendix 3). On hollows (4.9–8.0 mg m<sup>-2</sup>h<sup>-1</sup>) and high lawns (4.4–5.4 mg m<sup>-2</sup>h<sup>-1</sup>) the emissions were significantly greater than those on high hummocks (2.1–2.8 mg m<sup>-2</sup>h<sup>-1</sup>). In August, the mean CH<sub>4</sub> flux was highest on the sampled hummock (7.67 mg m<sup>-2</sup>h<sup>-1</sup>), and the hollow (3.89 mg m<sup>-2</sup>h<sup>-1</sup>) and the high lawn (3.30 mg m<sup>-2</sup>h<sup>-1</sup>) had much smaller fluxes. The nighttime measurement showed similar results, but the difference between the flux from the high hummock and the hollow/high lawn was less than that in the daytime measurements.

Table 1. Mean, standard deviation, minimum and maximum of methane fluxes from different microsites from May to July, and the total mean flux for the ombrotrophic bog based on sampled plots. The values in parenthesis include measurements from August, which do not represent the microsite types as effectively as the measurements from May to July.

	CH <sub>4</sub> flux (mg m <sup>-2</sup> d <sup>-1</sup> )				
	Mean	SD	Min	Max	n
<b>Microsite</b>					
HO	151 (136)	63 (71)	34 (28)	209 (209)	8 (12)
HL	118 (110)	58 (57)	40 (22)	249 (249)	9 (13)
HHU	53 (93)	26 (66)	14 (14)	84 (209)	9 (13)
<b>Total:</b>	108 (113)				27 (35)

n denotes the number of closed chamber measurements that yielded results in flux calculations

During the growing period, the peat temperatures ranged from 11.0 to 18.4 °C (depth of 5 cm), 9.9 to 17.9 °C (15 cm), and 8.7 to 18.9 °C (30 cm). At each depth, only limited variation could be observed between microsites (Table 2).

Water table levels at the microsites varied very little during the growing period. The average water table levels were highest on hollows (+4 cm), intermediate on high lawns (-10 cm), and lowest on high hummocks (-19 cm) (Table 3). The monthly variations in water table levels are presented at Figure 8.

Table 2. Monthly flux measurements and environmental parameters at each microsite on the bog: average flux, average water table position and average peat temperature at different depths. For August, the water table levels shown here are only from the sampled plots, as they are related to the measured flux.

Month	Microsite	Flux	WT	T(°C)	T(°C)	T(°C)
		(mg m <sup>-2</sup> h <sup>-1</sup> )	(cm)	5 cm	15 cm	30 cm
May	HO	4.9	2.3	11.3	9.9	9.3
	HL	4.4	-11.3	11.4	9.9	8.8
	HHU	2.2	-21.3	11.0	9.5	8.7
June	HO	5.5	6.7	17.7	15.7	14.6
	HL	4.8	-10.7	18.4	15.9	14.3
	HHU	1.5	-22.0	18.0	15.7	14.0
July	HO	8.0	2.7	15.4	14.9	15.1
	HL	5.5	-9.3	15.6	14.9	14.6
	HHU	2.9	-18.7	14.6	14.3	14.6
August	HO	3.9	3.0	14.3	12.9	13.1
	HL	3.3	-7.0	14.8	14.8	14.9
	HHU	7.7	-15.0	14.1	14.3	14.9
August night	HO	5.6	3.0	15.1	16.1	15.1
	HL	5.5	-7.0	14.1	14.3	16.2
	HHU	7.3	-15.0	18.1	17.9	18.9

Table 3. Mean, standard deviation, minimum and maximum of water table levels at each microsite on the bog from May to August. Negative values are below and positive above the peat surface.

Microsite	Water table (cm)				
	Mean	SD	Min	Max	n
HO	4	3	-1	10	12
HL	-10	3	-14	-7	12
HHU	-19	4	-26	-13	12
<b>Total:</b>					36

---

n denotes the number of measurement times

---

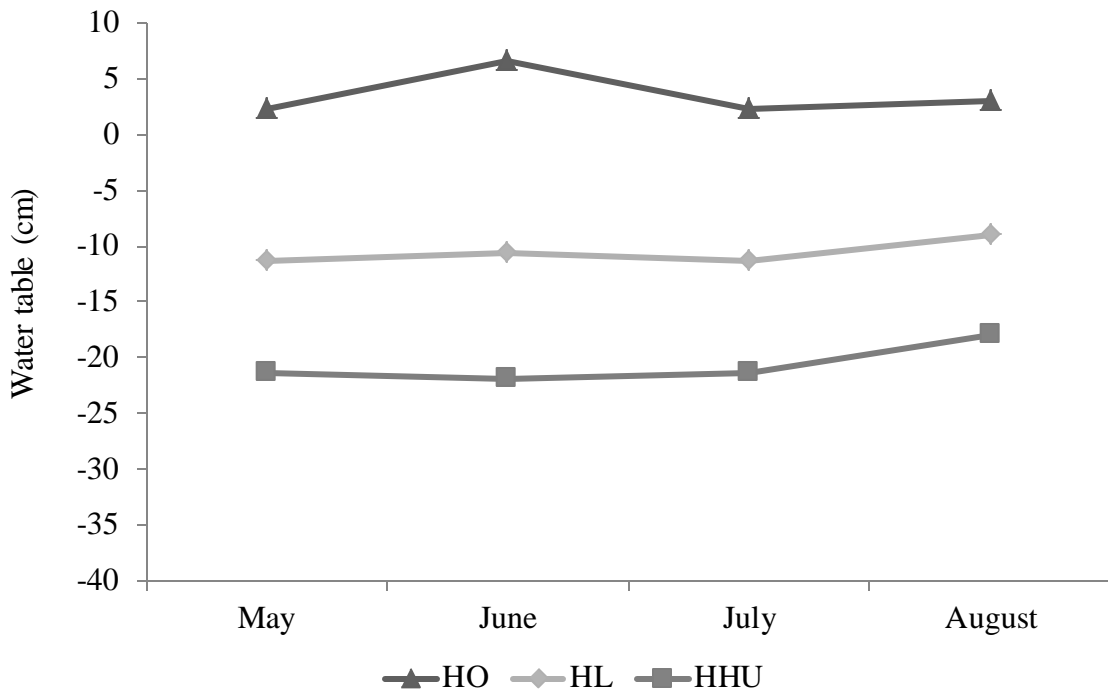


Figure 8. Monthly changes in water table levels at each microsite on the bog.

### 5.1.2. Fen

Throughout the growing period, all samples from the hollows and lawns had positive mean  $\text{CH}_4$  flux values ranging from 52 to 160  $\text{mg m}^{-2}\text{d}^{-1}$ . In July and August, some hummocks had negative flux rates ranging from -13 to -3  $\text{mg m}^{-2}\text{d}^{-1}$ . The  $\text{CH}_4$  emissions were the highest on hollows and the lowest on hummocks. The mean  $\text{CH}_4$  fluxes are represented by two values in Table 4; the first values are the results from May to July, and the values in parenthesis are the results from May to August, also including the non-repetitive night measurements. Three chamber measurements from the hummocks were discarded as poor quality of data, because calculating the flux was impossible. Without the data from August, the mean  $\text{CH}_4$  flux from *Carex* lawns is less than the mean flux from hummocks.



Table 4. Mean, standard deviation, minimum and maximum of methane fluxes from different microsites from May to July, and the total mean flux of the minerotrophic fen. The values in parenthesis include measurements from August, which do not represent the microsite types as effectively as the measurements from May to July.

	<b>CH<sub>4</sub> flux (mg m<sup>-2</sup>d<sup>-1</sup>)</b>				
	Mean	SD	Min	Max	n
<b>Microsite</b>					
HO	97 (160)	54 (117)	38 (38)	189 (417)	9 (13)
CR	52 (78)	17 (86)	23 (23)	78 (359)	9 (13)
HU	67 (58)	149 (126)	-3 (-13)	371 (371)	6 (9)
<b>Total:</b>	72 (99)				24 (35)

n denotes the number of closed chamber measurements that yielded results in flux calculations

In May, the highest flux was from the hummocks (7.8 mg m<sup>-2</sup>h<sup>-1</sup>), and the fluxes from the hollows (2.5 mg m<sup>-2</sup>h<sup>-1</sup>) and *Carex* lawns (1.4 mg m<sup>-2</sup>h<sup>-1</sup>) were significantly less (Table 5). From June to August, the mean emission rates decreased in the order of hollows > *Carex* lawns > hummocks. The average flux ranged from 3.1 to 13.7 mg m<sup>-2</sup>h<sup>-1</sup> on the hollows, from 2.2 to 15.0 mg m<sup>-2</sup>h<sup>-1</sup> on *Carex* lawns, and from -0.4 to 5.9 mg m<sup>-2</sup>h<sup>-1</sup> on the hummocks.

During the growing period, the peat temperatures ranged from 6.3 to 26.2 °C (depth of 5 cm), 7.6 to 17.4 °C (15 cm), and 10.2 to 15.8 °C (30 cm). At each depth, only limited variation could be observed between microsites (Table 5).

Water table levels at the microsites varied very little during the growing period. The average water table levels were highest on hollows (-10 cm), intermediate on high lawns (-12 cm), and lowest on high hummocks (-29 cm) (Table 6). Measured water table levels from the hollows and *Carex* lawns overlap each other, because the microsite's differentiation is mainly derived from dominating plant communities. The monthly variations in water table levels are presented in Figure 9.

Table 5. Monthly flux measurements and environmental parameters at each microsite on the fen: average flux, average water table position and average peat temperature at different depths. For August, the water table levels shown here are only from the sampled plots, as they are related to the measured flux.

Month	Microsite	Flux	WT	T(°C)	T(°C)	T(°C)
		(mg m <sup>-2</sup> h <sup>-1</sup> )	(cm)	5 cm	15 cm	30 cm
May	HO	2.5	-9.3	12.4	11.3	10.2
	CR	1.4	-12.3	13.0	12.1	10.6
	HU	7.8	-27.0	14.0	12.8	11.9
June	HO	3.1	-9.0	17.0	16.4	14.4
	CR	2.6	-12.7	16.6	16.6	14.7
	HU	0.9	-26.0	17.6	15.7	15.5
July	HO	6.9	-7.7	19.6	17.4	15.4
	CR	2.2	-10.0	19.2	17.4	15.4
	HU	0.1	-25.3	19.3	17.4	15.8
August	HO	12.2	-13.0	19.5	15.3	15.6
	CR	3.0	-14.0	18.2	15.0	14.5
	HU	-0.4	-37.0	26.2	15.5	14.5
August night	HO	13.7	-13.0	13.1	15.4	14.8
	CR	15.0	-14.0	6.3	7.6	15.4
	HU	5.9	-37.0	10.0	10.7	10.3

Table 6. Mean, standard deviation, minimum and maximum of water table levels at each microsite from May to August at the fen. Negative water table levels are below the peat surface.

Microsite	Water table (cm)				
	Mean	SD	Min	Max	n
HO	-10	3	-13	-6	10
CR	-12	3	-16	-7	10
HU	-29	7	-37	-18	8
<b>Total:</b>					29

n denotes the number of measurement times

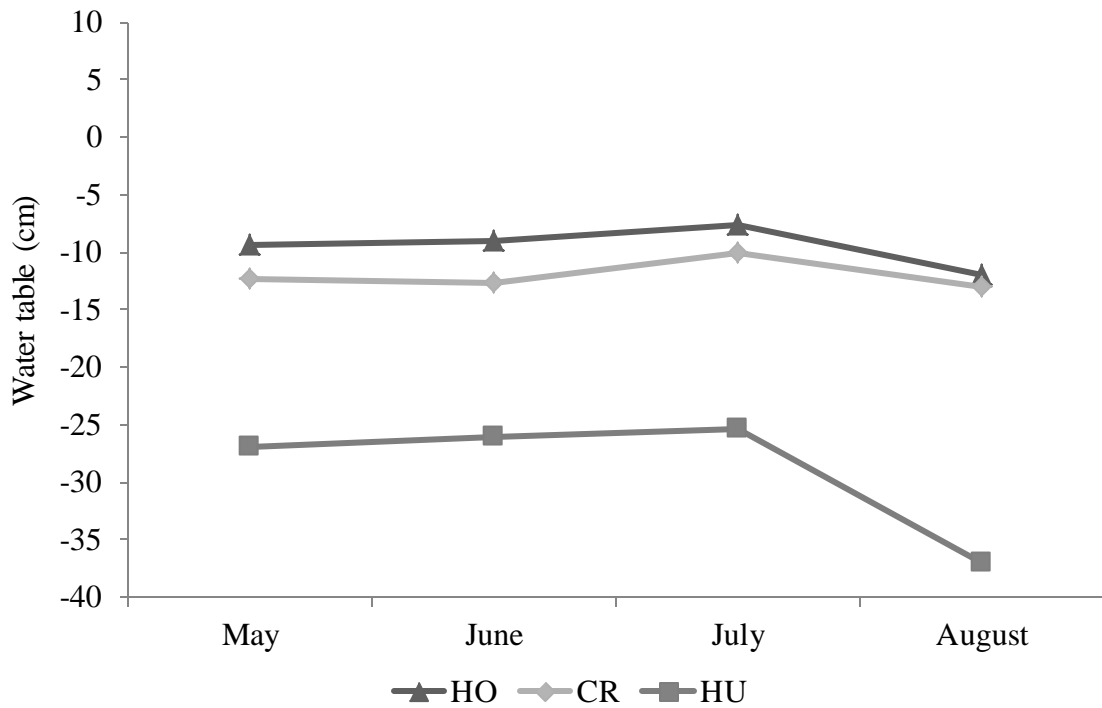


Figure 9. Monthly changes in water table levels at each microsite on the fen.

## 5.2. Isotope results of emitted methane

### 5.2.1 Bog

The  $\delta^{13}\text{C}_{\text{CH}_4}$  results of the emitted methane ranged from -71.5 to -52.2 ‰ (Table 7). During the growing period, the mean  $\delta^{13}\text{C}_{\text{CH}_4}$  source signatures from  $\text{CH}_4$  emissions were more negative at the hollows (-67.4 ‰) and high lawns (-66.4 ‰) than at the hummocks (-63.4 ‰), and the mean source signature for the site was -66.0 ‰. The correlation coefficient was the lowest at high hummocks with  $R^2 = 0.59$ , and the highest at high lawns with  $R^2 = 0.79$ . The Keeling plots showing the source signature at each microsite from May to August, are presented in Figure 10. The used background values of  $\text{CH}_4$  concentration and  $\delta^{13}\text{C}_{\text{CH}_4}$  are the global means ( $c_{\text{CH}_4} = 1.8$  ppm and  $\delta^{13}\text{C}_{\text{CH}_4} = -47.4$  ‰). The Keeling plot for the site is at Appendix 2.

Table 7. Mean  $\delta^{13}\text{C}$  source signature of each microsite from May to August at the bog. Source signature is the intercept of y-axis in the Keeling plot geometric mean regression. The uncertainty is the standard error in the intercept.  $R^2$  is the correlation coefficient between  $\text{CH}_4$  concentration and  $\delta^{13}\text{C}$ .

	$\delta^{13}\text{C}$ source signature				
	$\delta^{13}\text{C}$ (‰)	$\pm$ (‰)	$R^2$	range (‰)	n
<b>Microsite</b>					
HO	-67.4	1.1	0.76	-70.6 to -55.2	23
HL	-66.4	0.8	0.79	-71.5 to -57.6	22
HHU	-63.4	1.5	0.59	-69.2 to -52.2	23
tot:	-66.0	0.7	0.70		68

n denotes the number of successful  $\delta^{13}\text{C}$  analysis

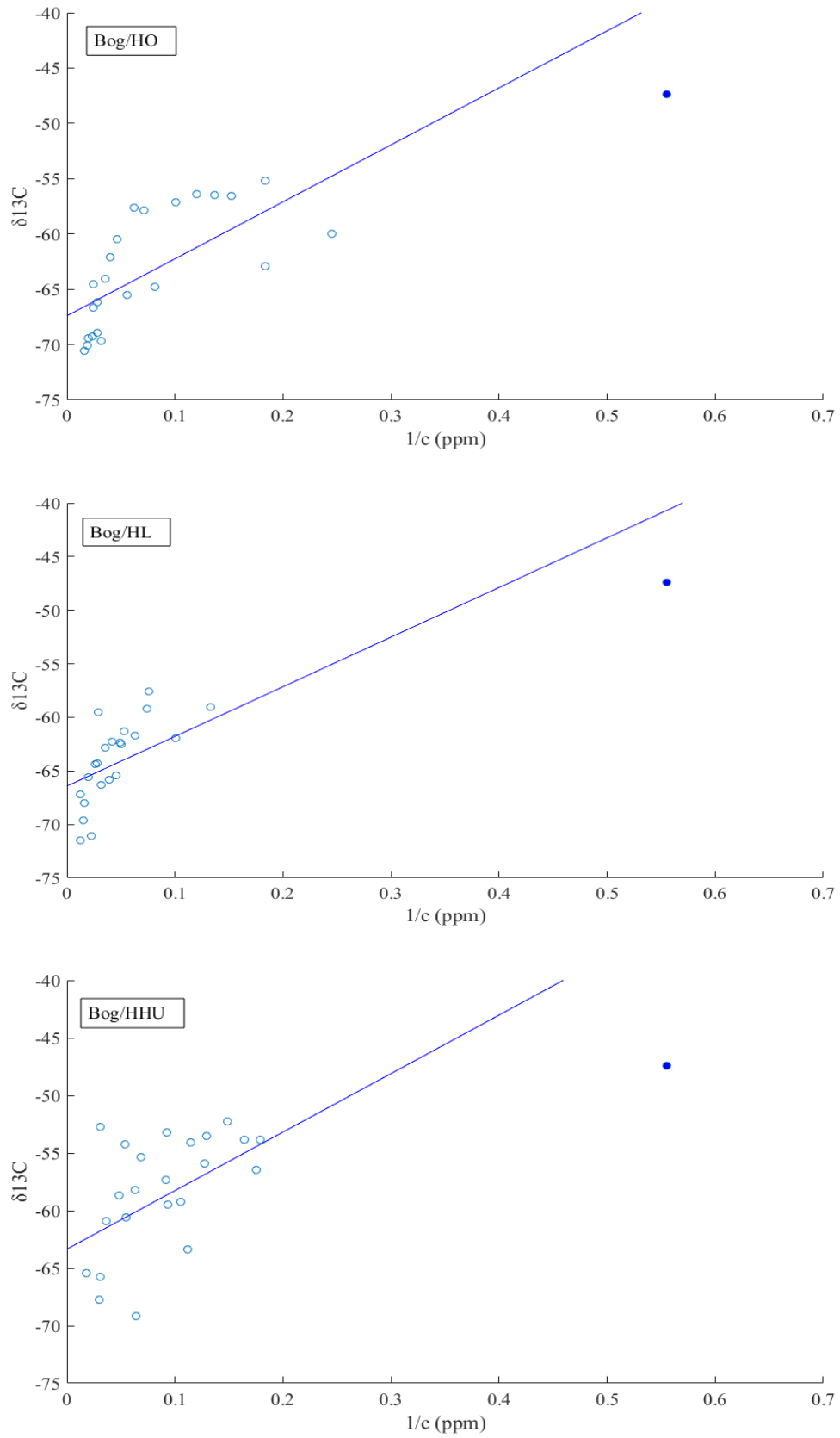


Figure 10. Keeling plots showing the mean source signature (y-axis intercept) of  $CH_4$  on each microsite from May to August at the bog. Filled circles represents the background values.

The monthly variations in mean  $\delta^{13}\text{C}$  source signatures at the site were from -67.7 to -62.6 ‰ being most negative in July (Table 8a). The correlation coefficient was lowest ( $R^2 = 0.6$ ) in August, though all the samples were drawn from the same set of plots. The highest correlation was in May ( $R^2 = 0.82$ ), not including the non-repetitive night samples. Table 8b shows the  $\delta^{13}\text{C}$  source signature for each microsite from May to August. At all microsities, the  $\delta^{13}\text{C}$  was most negative in July and least negative in May. In August, only hummock showed diurnal variation beyond margin of error, but is based on one sample only and thus not reliable.

Table 8. a) Mean  $\delta^{13}\text{C}$  source signature of ombrotrophic bog from May to August. Source signature is the intercept of y-axis in the Keeling plot linear regression. The uncertainty is the standard error in the intercept.  $R^2$  is the correlation coefficient between  $\text{CH}_4$  concentration and  $\delta^{13}\text{C}$ . b)  $\delta^{13}\text{C}$  source signature of each microsite from May to August.

a) Source signature per month						
	$\delta^{13}\text{C}$ (‰)	$\pm$ (‰)	$R^2$	range (‰)	n	
<b>Month</b>						
May	-62.6	1.1	0.82	-64.1 to -53.2	15	
June	-66.0	1.3	0.75	-71.0 to -53.5	18	
July	-67.7	1.7	0.74	-71.5 to -54.2	13	
August	-64.6	1.6	0.63	-69.6 to -52.2	17	
August night	-67.5	1.3	0.95	-69.7 to -62.3	5	
tot:	-66.0	0.7	0.70		69	
b) Source signature per month per microsite						
Microsite	HO		HL		HHU	
	$\delta^{13}\text{C}$ (‰)	$\pm$ (‰)	$\delta^{13}\text{C}$ (‰)	$\pm$ (‰)	$\delta^{13}\text{C}$ (‰)	$\pm$ (‰)
<b>Month</b>						
May	-62.1	1.2	-63.9	0.5	-58.9	1.8
June	-67.0	1.9	-67.2	1.4	-59.2	1.1
July	-70.0	0.7	-67.0	2.5	-64.6	3.4
August	-64.6	2.6	-65.7	1.9	-61.7	2.7
August night	-69.4	1.7	-64.5	0.7	-68.9	-
n denotes the number of successful $\delta^{13}\text{C}$ analysis						

### 5.2.2. Fen

During the growing period, the mean  $\delta^{13}\text{C}_{\text{CH}_4}$  source signature was more negative at the hollows (-64.5 ‰) and *Carex* lawns (-64.1‰) than at the hummocks (-62.9 ‰), though the difference is within the margin of error (Table 9). The mean source signature of the site was -63.2 ‰. The correlation coefficient of the Keeling plot varied from 0.7 to 0.8. The Keeling plots showing the source signature at each microsite from May to August are presented in Figure 11, and the used background values of  $\text{CH}_4$  concentration and  $\delta^{13}\text{C}_{\text{CH}_4}$  are the global means ( $c_{\text{CH}_4} = 1.8$  ppm and  $\delta^{13}\text{C}_{\text{CH}_4} = -47.4$  ‰). The Keeling plot for the site is at Appendix 2.

Table 9. Mean  $\delta^{13}\text{C}$  source signature on each microsite from May to August at the fen. Source signature is the intercept of y-axis in the Keeling plot linear regression. The uncertainty is the standard error in the intercept.  $R^2$  is the correlation coefficient between  $\text{CH}_4$  concentration and  $\delta^{13}\text{C}$ .

	$\delta^{13}\text{C}$ source signature				
	$\delta^{13}\text{C}$ (‰)	$\pm$ (‰)	$R^2$	range (‰)	n
<b>Microsite</b>					
HO	-64.5	1.0	0.76	-69.6 to -51.1	23
CR	-64.1	1.6	0.66	-70.0 to -48.1	23
HU	-62.9	1.8	0.78	-66.4 to -44.8	22
tot:	-63.2	0.8	0.77		68
n denotes the number of successful $\delta^{13}\text{C}$ analysis					

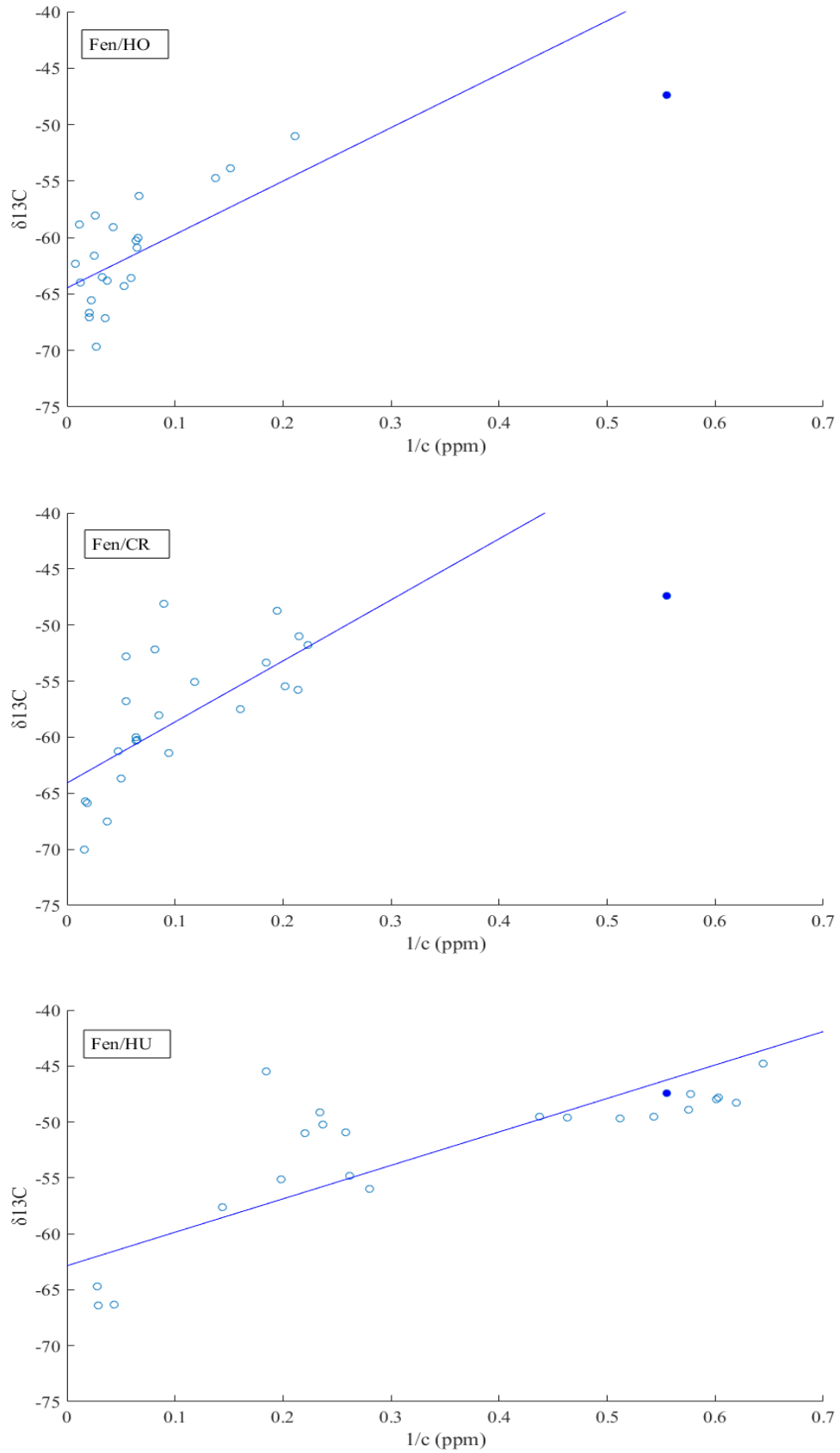


Figure 11. Keeling plots showing the mean source signature (y-axis intercept) of  $\text{CH}_4$  at each microsite from May to August. Filled circles represents the background values.



The monthly variations in the mean  $\delta^{13}\text{C}$  source signatures at the site ranged from -67.6 to -60.13 ‰ (Table 10a). The correlation coefficient was the lowest ( $R^2 = 0.6$ ) in August, owing to the very low correlation at the hummocks ( $R^2 = 0.15$ ) (Appendix 3), because the  $\text{CH}_4$  concentration levels in the some chambers did not change distinctively from the atmospheric background level. All results from hummocks are still included, though differentiating source signature from ambient atmospheric  $\delta^{13}\text{C}_{\text{CH}_4}$  could be impossible, in cases of very low flux rate (Dorodnikov et al. 2012). Table 10b shows the  $\delta^{13}\text{C}$  source signature for each microsite from May to August.

Table 10. a) Mean  $\delta^{13}\text{C}$  source signature of the minerotrophic fen from May to August. Source signature is the intercept of y-axis in the Keeling plot linear regression. The uncertainty is the standard error in the intercept.  $R^2$  is the correlation coefficient between  $\text{CH}_4$  concentration and  $\delta^{13}\text{C}$ . b)  $\delta^{13}\text{C}$  source signature of each microsite from May to August.

a)					
Source signature per month					
	$\delta^{13}\text{C}$ (‰)	$\pm$ (‰)	$R^2$	range (‰)	n
<b>Month</b>					
May	-61.3	1.6	0.77	-66.4 to -48.9	14
June	-63.8	1.0	0.88	-67.0 to -49.5	18
July	-65.7	1.0	0.97	-69.6 to -44.8	14
August	-60.1	1.8	0.61	-62.3 to -45.5	16
August night	-67.6	1.0	0.96	-70.0 to -64.0	6
tot:	-63.2	0.8	0.77		68

b)						
Source signature per month per microsite						
Microsite	HO		CR		HU	
	$\delta^{13}\text{C}$ (‰)	$\pm$ (‰)	$\delta^{13}\text{C}$ (‰)	$\pm$ (‰)	$\delta^{13}\text{C}$ (‰)	$\pm$ (‰)
<b>Month</b>						
May	-60.3	2.4	-59.8	2.1	-64.8	4.1
June	-64.8	1.3	-63.1	1.7	-58.8	2.1
July	-68.3	1.7	-63.4	0.9	-61.9	4.8
August	-61.3	0.8	-55.1	2.2	-60.2	7.9
August night	-65.9	1.5	-69.9	0.9	-66.8	1.2

n denotes the number of successful  $\delta^{13}\text{C}$  analysis

### 5.3 The isotopes of DIC

#### 5.3.1 Bog

The pore water  $\delta^{13}\text{C}_{\text{DIC}}$  samples collected at the depth of 50 cm varied during the growing period (Table 11), and ranged from -4.1 to 3.6 ‰. In May the mean  $\delta^{13}\text{C}_{\text{DIC}}$  was from -4.1 to 1.8 ‰, in July from -0.7 to 1.7 ‰, and in August from -1.1 to 3.0 ‰. At hollows,  $\delta^{13}\text{C}_{\text{DIC}}$  values were positive each month ranging from 0.6 to 3.0 ‰. At the hummocks,  $\delta^{13}\text{C}$  values were always negative ranging from -4.1 to -0.7 ‰. The mean  $\delta^{13}\text{C}_{\text{DIC}}$  for the site ranged from -1.5 ‰ in May to 1.3 ‰ in August.

Table 11. Mean, standard deviation, minimum and maximum of  $\delta^{13}\text{C}_{\text{DIC}}$  from different microsites and per site, in May, July and August at the bog.

Microsite	$\delta^{13}\text{C}_{\text{DIC}}$ per month per microsite				n
	Mean (‰)	SD	Min (‰)	Max (‰)	
May					
HO	1.8	0.0	1.7	1.8	2
HL	-2.2	0.0	-2.2	-2.2	2
HHU	-4.1	0.0	-4.1	-4.1	2
tot:	-1.5				6
July					
HO	0.6	0.6	0.2	1.2	3
HL	1.7	0.0	1.7	1.7	3
HHU	-0.7	0.2	-0.9	-0.4	3
tot:	0.5				9
August					
HO	3.0	0.5	2.4	3.6	6
HL	2.0	0.3	1.6	2.4	6
HHU	-1.1	0.7	-1.8	-0.4	6
tot:	1.3				18

## 5.3.2. Fen

The pore water  $\delta^{13}\text{C}_{\text{DIC}}$  samples collected at the depth of 50 cm varied greatly during the growing period, and all the values were negative (Table 12). In May the mean  $\delta^{13}\text{C}_{\text{DIC}}$  was from -18.5 to -4.5 ‰, in July from -9.9 to -3.9 ‰, and in August from -7.9 to -0.4 ‰. Each month, the  $\delta^{13}\text{C}$  was the most negative at different microsite. The monthly mean for the site was the most negative in May (-12.6 ‰) and the least negative in August (-3.7 ‰).

Table 12. Mean, standard deviation, minimum and maximum of  $\delta^{13}\text{C}_{\text{DIC}}$  from different microsities and per site, in May, July and August at the fen.

Microsite	$\delta^{13}\text{C}_{\text{DIC}}$ per month per microsite				n
	Mean (‰)	SD	Min (‰)	Max (‰)	
May					
HO	-18.5	0.2	-18.7	-18.4	2
CR	-14.8	0.6	-15.2	-14.4	2
HU	-4.5	0.1	-4.6	-4.4	2
tot:	-12.6				6
July					
HO	-3.9	1.6	-6.0	-3.0	3
CR	-7.0	0.9	-10.0	-7.4	3
HU	-9.9	0.4	-10.1	-2.9	3
tot:	-6.9				9
August					
HO	-0.4	0.2	-0.8	-0.1	6
CR	-7.9	0.3	-8.2	-7.5	6
HU	-1.8	0.1	-1.9	-1.7	3
tot:	-3.7				15

## 6. DISCUSSION

### 6.1. Effect of microtopography on methane emissions

#### 6.1.1. Bog

On the bog, all microsites acted as sources of atmospheric methane during the growing period. The average rate of emitted CH<sub>4</sub> was affected by microtopography, as the highest flux was from water-saturated hollows, and the lowest flux was from elevated hummocks (Table 1). All sampled microsite types showed temporal and spatial variation.

At each microsite, the water table levels had distinctive values which varied only little on a monthly scale (Fig. 8). Despite the site's pronounced microtopography, the monthly mean CH<sub>4</sub> emissions do not show correlation to the average water table position (Fig. 12). Even without the less presentative August measurements, the flux rates from hollows and lawns are too concurrent to show correlation with water table levels, though high hummocks then display significantly lower flux rates compared to hollows and high lawns (Fig. 13). This indicates that the water table position, and therefore the thickness of the oxidation zone, is not a controlling factor to the large scale summer time CH<sub>4</sub> emission at the site, though it can override other factors by contributing to the smaller scale variations especially at elevated hummocks.

Many other studies have shown the water table position to be the main controlling factor of CH<sub>4</sub> emissions at northern peatlands (e.g. Bubier et al. 1995, MacDonald et al. 1998, Dorodnikov et al. 2013). However, Christensen et al. (2003a) identify water table position around or above -10 cm to be sort of a threshold, as other processes take over the control on larger scale variability at these relatively wetter sites.

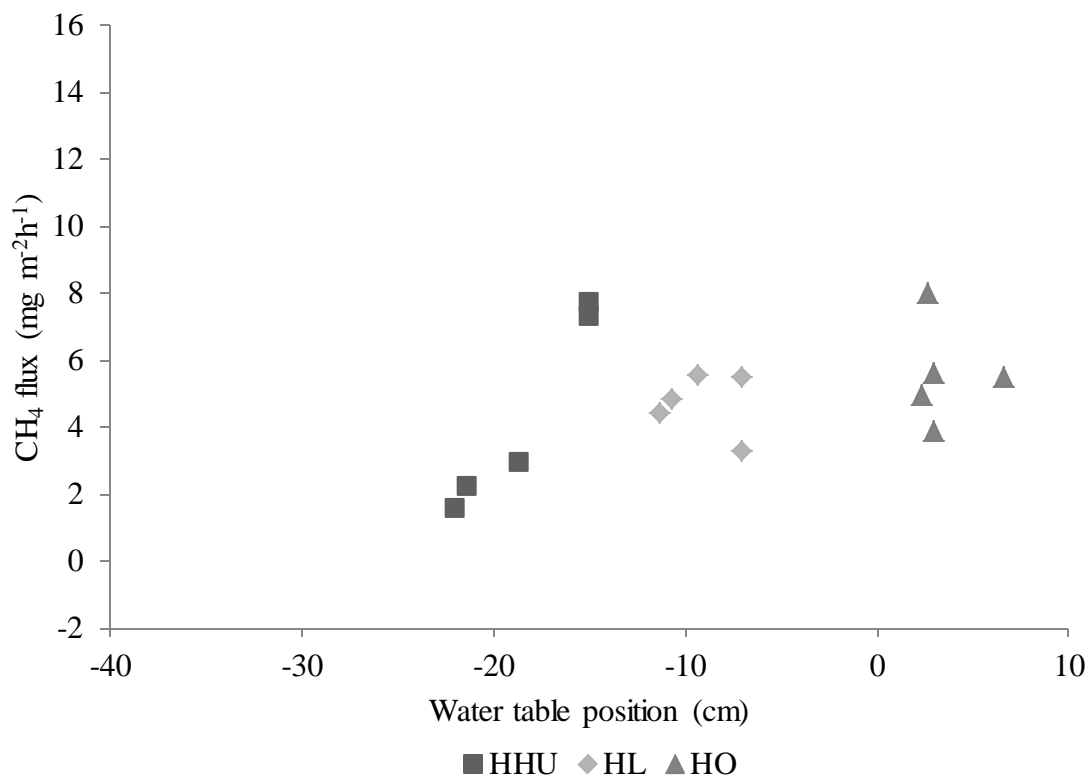


Figure 12. The monthly CH<sub>4</sub> fluxes of each microsite at the bog relative to the average water table position.

The water table level rose from July to August, though August 2015 received so little precipitation compared to a 30-yr monthly average (Fig. 3 and 8). As the bog is not connected to the surrounding groundwater system, the water table levels are independent from changes in groundwater levels which are affected by the amount of rainfall in the catchment area. It is also noteworthy that the water table position does not change in concert with between the microsites, as June displays the maximum and August the minimum of differences between measured water table levels. A monthly interval in measurements is not sufficient to make conclusions about the driving mechanism behind this pattern if there is such. Uljas (2015) reported water table position data from the same measurement site from the growing periods of 2012 and 2013. The data showed significant (approx.  $\pm 4$  cm) variation on a shorter time scale at each microsite, but the changes were concurrent with one another.

Figure 13 displays the monthly variation in the CH<sub>4</sub> fluxes, and the peat temperatures at the depths of 5, 15 and 30 cm. At the depth of 30 cm, the temperatures are least susceptible to diurnal air temperature variations and follow the changes of the average

monthly air temperatures (Fig. 2). At none of the microsites, the CH<sub>4</sub> fluxes show direct correlation to the peat temperatures, though the mean CH<sub>4</sub> flux rate and temperature both rose till high summer. On a monthly scale, the hollows and the high lawns showed growing trend in CH<sub>4</sub> emissions from May to July, and the emissions from the hummocks were significantly lower. This changed in August as the highest emission was at the hummock, and emissions at hollow and lawn dropped to their lowest values during the measurement period. Aside not being as representable as other months, the August emissions at hollow and lawn could result from changes in net ecosystem production (NEP) and labile substrate availability owing to the growing period evolutions in plant communities. Uljas (2015) reported NEP results from the same study site, which show a declining trend towards the end of the growing period, as the vegetation start to senesce and the plant productivity goes down. At hummocks, it is possible that the growth and development of vascular plants towards end-of-season is responsible of increase in their CH<sub>4</sub> emissions (Heikkinen et al. 2002).

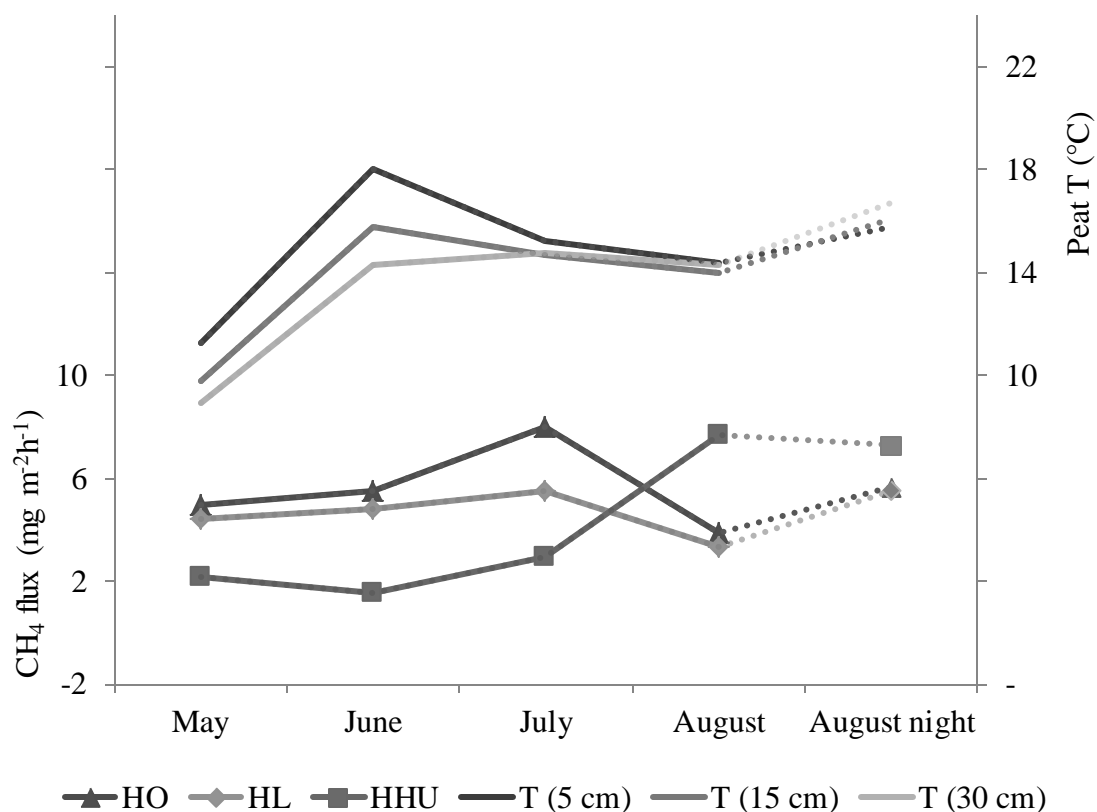


Figure 13. Monthly variation in CH<sub>4</sub> flux at each microsite of the bog, and peat temperature changes at the depths of 5, 15 and 30 cm. Results from August nighttime measurements are included with dashed lines.

In August, the nighttime emissions were clearly higher at hollow and lawn than during the day. This is most likely due to the complex role of plants in the production and transport of CH<sub>4</sub> in the peat. E.g. the lack of photosynthesis in upper biomass during nighttime combined to anaerobic plant respiration typical to certain vegetation communities that produces methane (Clymo 1984).

### 6.1.2. Fen

On the fen, the microtopography is less pronounced than at the bog. During the growing period, the highest emissions were from hollows and the lowest from hummocks (including the August results) and the site acted as a source of atmospheric methane. The flux was negative at one plot of hummocks in July and at each hummock sampled in August, and these plots acted as sinks of methane. Observed flux rates are consistent with other studies (e.g. Moore and Knowles 1990, Rinne et al. 2007, Riutta et al. 2007). Riutta et al. conducted chamber measurements at the same site and observed similar fluxes from all microsites. However, their study had three different types of lawns (*Carex rostrate*, *C. lasiocarpa* and *Eriophorum vaginatum*) from which *Carex lasiocarpa* demonstrated almost as high a flux as that at hollows, indicating large variations between different types of lawn surfaces.

The difference between water table position at the hollows and *Carex* lawns is only few centimeters, as the microsite types are mostly differentiated by the dominating vegetation. Water table levels did not show correlation with the CH<sub>4</sub> flux rates, probably because the variation in the monthly flux rates was significant (Fig. 14). From May to July, changes in the mean water table levels were very small. In August, the water table levels reflected the areas low precipitation, especially at the hummocks (Fig. 9). All the monthly changes were aligned with one another, as the changes in water table levels were consistent within the microsites. This indicates that the water table levels were independent from vegetation type at each microsite.

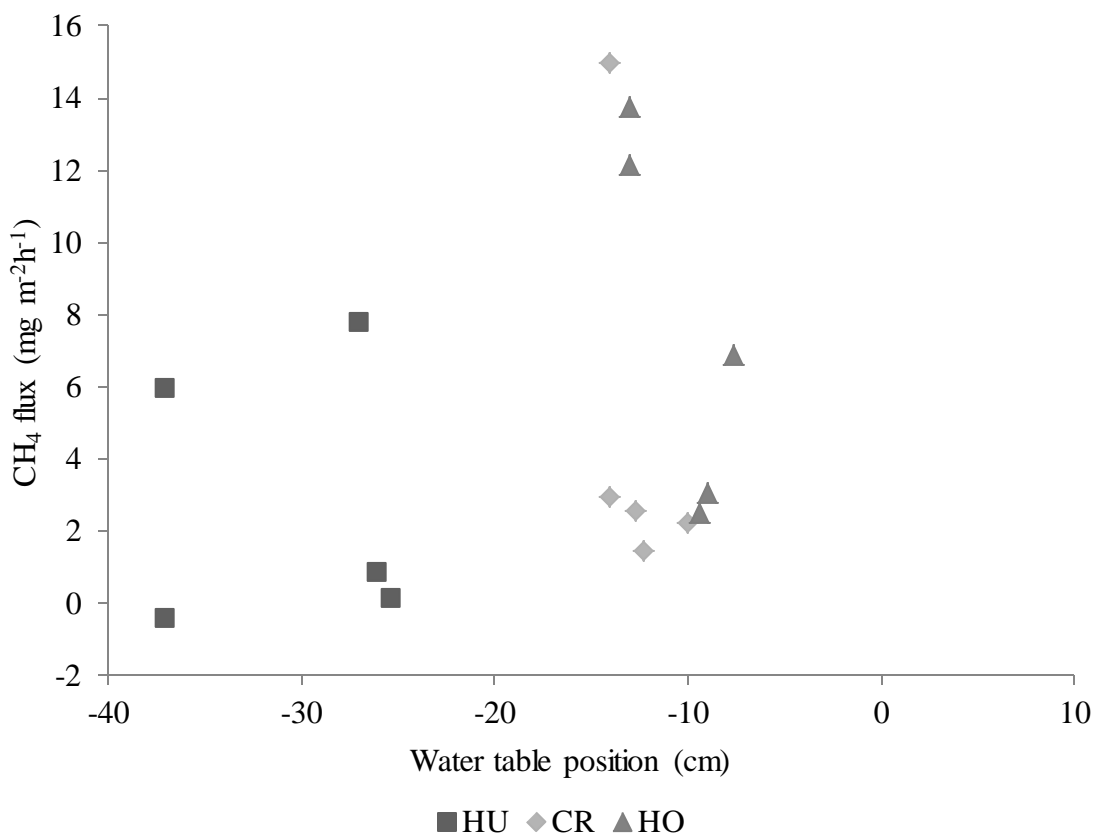


Figure 14. The monthly CH<sub>4</sub> fluxes of each microsite at the fen relative to the average water table position.

Figure 15 displays monthly changes in the CH<sub>4</sub> fluxes, and the peat temperatures at the depths of 5, 15 and 30 cm. At all microsites, the peat temperatures at the depth of 5 cm were measured above water table level, and thus very susceptible to diurnal temperature variations. Only emissions at the hollows showed dependence on the peat temperature at the depth of 5 cm, whereas the mean emissions from the *Carex* lawns and hummocks had more narrow scale variation. In May, the hummocks are an exception, as the mean emission is much higher than encountered in other months. However, the mean was derived from two chamber measurements which displayed highly different CH<sub>4</sub> fluxes, 0.1 and 15.4 mg m<sup>-2</sup>h<sup>-1</sup> (Appendix 3). The higher flux is most likely due to ebullition, which is unaffected by the methanotrophs' oxidation. Rinne et al. (2007) found no dependence between CH<sub>4</sub> emissions and peat temperature, during the high and late summer at the Siikaneva fen, possibly owing to the limited substrate availability (Chasar et al. 2000a).



In August, there was a huge difference in daytime and nighttime emissions, especially at *Carex* lawn and hummock. This was most likely due to the relatively large temporal variation in the emissions recorded at the site. In the eddy covariance measurements, systematic diurnal variation was not found from the CH<sub>4</sub> emissions (Rinne et al. 2007). However, Mikkilä et al. (1995) reported from another boreal mire site a significant diurnal variation in CH<sub>4</sub> emissions during periods of high variation in solar radiation and peat temperature. They measured nighttime emissions to be 2-3 times higher than daytime emissions at drier plant communities, likely owing to the inhibition of CH<sub>4</sub> oxidation in the aerobic zone and the changes in substrate availability in the anaerobic zone. In their study, a similar trend was not found at wetter sites.

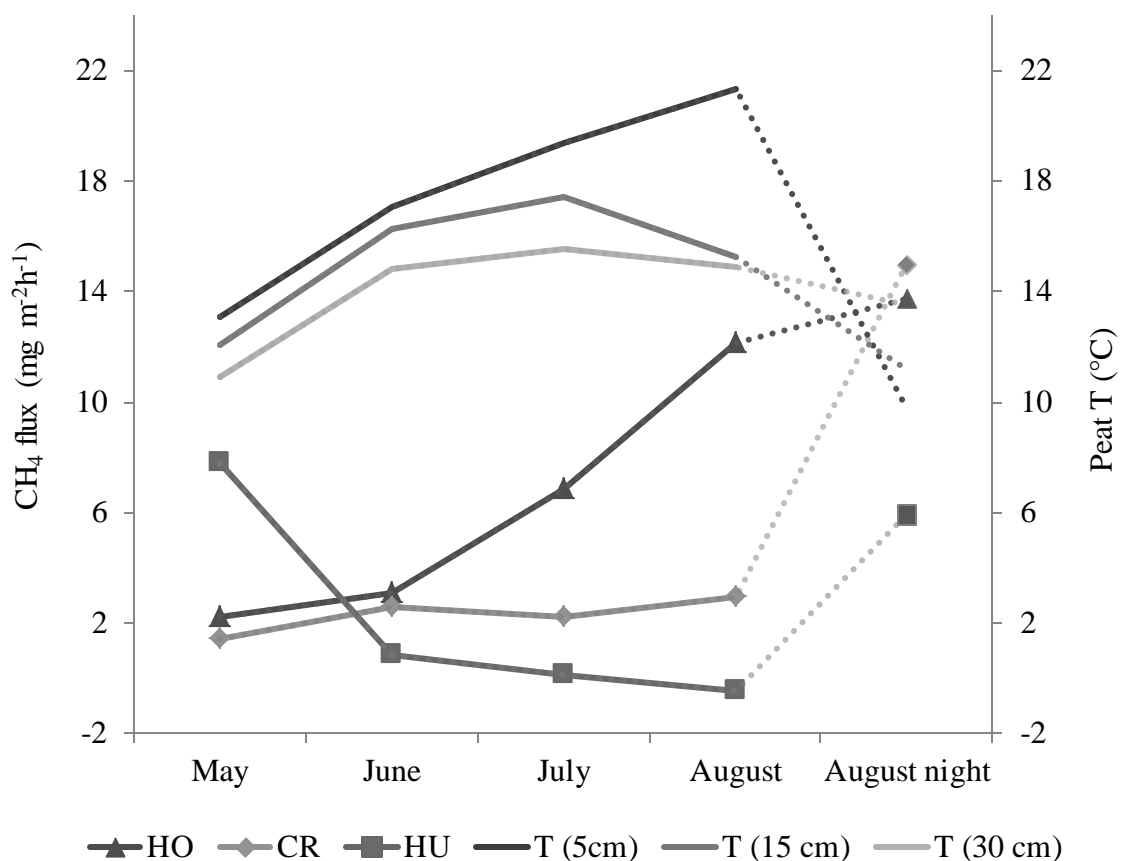


Figure 15. Monthly variation in CH<sub>4</sub> flux at each microsite of the fen, and peat temperature changes at the depths of 5, 15 and 30 cm. Results from nighttime measurements are included with dashed lines.

### 6.2.3. Source of methane, sink of carbon

The total summertime emission from the bog was on average  $110 \text{ mg m}^{-2}\text{d}^{-1}$  (Table 1). In general, bogs have been reported to have lower emissions than fens (Brown 1998). In Siikaneva, the summertime emissions showed an opposite trend, as at the fen the total summertime emission was on average  $85 \text{ mg m}^{-2}\text{d}^{-1}$  (Table 4). This is consistent with eddy covariance measurements made at the same site by Rinne et al. (2007). They reported a summertime mean emission of  $84 \text{ mg m}^{-2}\text{d}^{-1}$ . The higher emissions from the bog can be the result from high spatial variation between and within peatland ecosystems, as only three different (most microtopographically apart) microsites were selected to this study instead of all seven microsite types available at the site. According to Nykänen et al. (1998), the peatlands in southern and middle boreal Finland depict higher  $\text{CH}_4$  emissions than the northern peatlands in general, possible related to higher mean temperatures in northern Europe owing to the Gulf Stream.

Combining the flux data of this study to net carbon exchange (NEE) values of other studies (Aurela et al. 2007, Riutta et al. 2007, Uljas 2015) it seems that both the Siikaneva bog and fen are sinks of carbon during the growing period, as both sites act mainly as sinks of  $\text{CO}_2$  and the emission levels of  $\text{CH}_4$  release less carbon than what is accumulated. It is still unclear, if the Siikaneva mire complex is a carbon sink throughout the year, because comprehensive all year  $\text{CH}_4$  emission data have not been published yet. The fen is a source of  $\text{CH}_4$  throughout the year with an annual emission of  $12.6 \text{ g m}^{-2}$  (Rinne et al. 2007), and the annual uptake of  $\text{CO}_2$  is approx.  $200 \text{ g m}^{-2}$  (Aurela et al. 2007). Typically, Finnish mires are sinks of carbon (Minkkinen et al. 2002) at the current climate state, but a big open question is what happens when the climate changes. Identifying large (ecosystem) scale controlling factors on  $\text{CH}_4$  emissions is hard. Christensen et al. (2003a) reported that temperature and microbial substrate availability would best explain the large scale variations in the annual mean  $\text{CH}_4$  emissions, and Nykänen et al. (1998) observed that if the northern climate would be drying, lowering water table levels would have reducing impact on  $\text{CH}_4$  emissions at natural mires sites. However, changing climate would cause changes in vegetation communities at an ecosystem scale, and different types of plant communities contribute to carbon balance in various ways (Riutta et al. 2007).

### 6.3. Isotopic evidence on methane production, transport and oxidation

All the isotope results of this study were in line with the average  $\delta^{13}\text{C}$  value of the biogenic methane emitted from northern peatlands. As expected in the study hypothesis and shown in Figure 16, at the bog the  $\text{CH}_4$  emitted from the hollows and lawns showed more negative  $\delta^{13}\text{C}$  values than those from the elevated hummocks. This can be understood, as the key zone to methanogenesis is in the shallow depths of the water saturated layers of peat and there is less exposure to methane-oxidizing bacteria (Whiticar 1999). At the fen, the difference variation of  $\delta^{13}\text{C}$  between microsites was less systematic than at the bog (Figure 17). This was most likely due to higher plant productivity and different vegetation composition (more arenchymous vascular plants) at the fen compared to that at the bog. Dorodnikov et al. (2013) reported insignificant differences between  $\delta^{13}\text{C}$  of emitted  $\text{CH}_4$  from hollows and lawns at another boreal mire site in Finland. However, their study did not include the  $\delta^{13}\text{C}$  of emitted  $\text{CH}_4$  from hummocks due to the low flux rates, which made differentiating the source signature from ambient the atmospheric  $\text{CH}_4$  concentration unreliable.

In general, higher flux rates lead to signatures more depleted in  $^{13}\text{C}$  (Appendix 1). However, this is controversial to many other studies (e.g. Chanton et al. 1995, Bellisario et al. 1999, Hornibrook and Bowes 2007), as they observed enriched  $^{13}\text{C}$  source signatures produced (likely via acetate fermentation pathway) at sites with high  $\text{CH}_4$  fluxes owing to the abundance of organic material prompting  $\text{CH}_4$  emissions. This indicates that the differences in vegetation communities (and thus in microtopography) have an impact on  $\text{CH}_4$  emissions without altering the  $\delta^{13}\text{C}$  values of the flux, as most of the emitted methane is diffused through aerenchymatous tissue (Bowes and Hornibrook 2006). However, it is noteworthy that these other studies all encountered higher flux rates emitted from fens, and they all were conducted at sites located in other parts of northern peatlands than boreal Scandinavia.

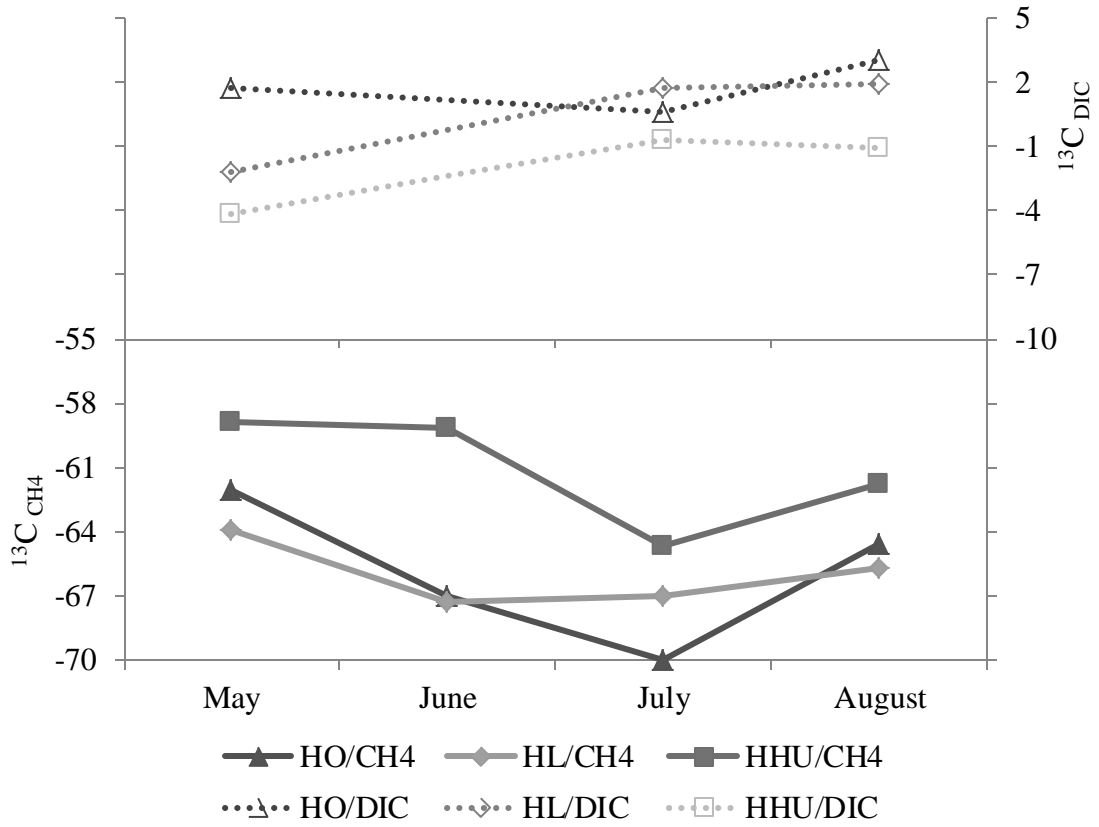


Figure 16. Monthly changes in isotopic composition of emitted CH<sub>4</sub> and pore water DIC at the bog.

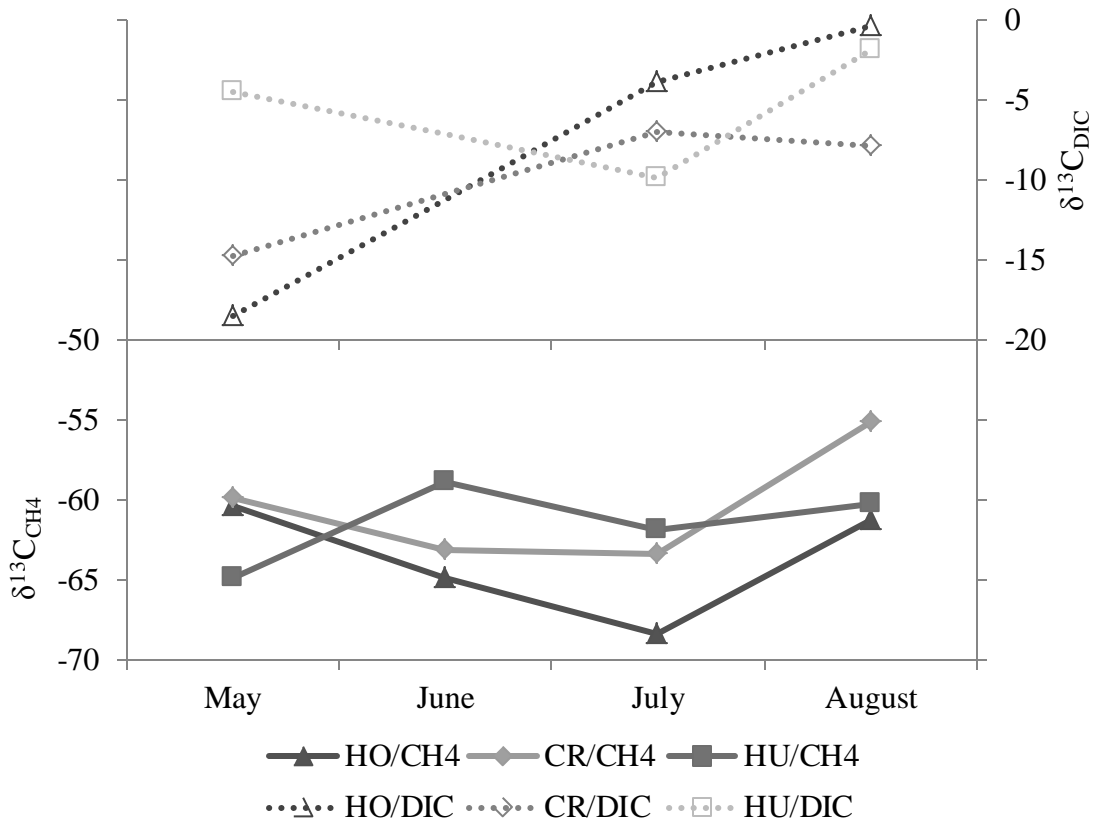


Figure 17. Monthly changes in isotopic composition of emitted CH<sub>4</sub> and pore water DIC at the fen.

At both sites, variations in  $\delta^{13}\text{C}$  at a monthly scale followed same pattern, as almost every microsite had the most negative  $\delta^{13}\text{C}$  in July. The observed variation in  $\delta^{13}\text{C}$  does correlate with alleged plant productivity during the growing period. Bellisario et al. (1999) did not observe any seasonal trend in  $\delta^{13}\text{C}$  values. However, their isotope samples were from the pore water and not from emission.

Part of the study hypothesis was that the methane production pathway would be different at the bog than at the fen, as the fen is more nutrient rich and should have more acetoclastic fermentation. Hence, it was expected that the isotope values would be more negative at the bog than at the fen. Results were consistent with the study hypothesis, and this indicates that the level of acetate fermentation is higher at the fen than at the bog. The average difference in  $\delta^{13}\text{C}$  between the sites was around 3 ‰, which is much less than in other studies that compare the isotope composition of  $\text{CH}_4$  from ombrotrophic bogs and minerotrophic fens. This is most likely due to the higher fluxes observed from the bog than from the fen. Also, the methane production pathways are driven by pH by inhibiting acetate utilization (Chanton et al. 2005) and the fen is quite acidic compared to pH range of fens in general, and there is no significant pH difference between the sites. Hornibrook (2009) gathered extensive data from several studies to his review and observed a significant depletion of  $^{13}\text{C}$  in the  $\text{CH}_4$  emission isotopes values collected from bogs ( $-74.9 \pm 9.8$  ‰) compared to those from fens ( $-64.8 \pm 4.0$  ‰). The review included samples collected from emission and pore water, and pore water samples showed an opposite trend compared to emissions, as more enriched  $\delta^{13}\text{C}$  values were observed from bogs.

Without the pore water samples of  $\text{CH}_4$  from the study sites, it is unconvincing to draw conclusions of the  $\text{CH}_4$  production pathways, as the concentration and the isotopic composition of  $\text{CH}_4$  changes in the vertical peat profile. As oxidation and acetate fermentation is largest in the upper part of the peat profile, pore water samples collected from this depth show significant increase in the  $\delta^{13}\text{C}$  values compared to those measured from emissions (Chanton et al. 2005, Dorodnikov et al. 2013). Dorodnikov et al. observed that the isotopic composition of  $\text{CH}_4$  in emission did not show significant difference to  $\delta^{13}\text{C}$  values at the depth of 1 m and deeper depths. This however does not conclusively mean that the at the deeper layers  $\text{CH}_4$  production is more driven by the

CO<sub>2</sub> reduction pathway, as the enrichment in the upper peat layer could be the result either from oxidation or acetate fermentation.

#### 6.4. DIC as an additional tool to identify CH<sub>4</sub> production pathways

At the pH range of the Siikaneva bog and fen, the major DIC species is dissolved CO<sub>2</sub> (Clark and Fritz 1997). DIC and DOC (dissolved organic carbon) are important components to determine the total C budget of the peatland ecosystem, as GHG (greenhouse gas) does not include them, and the GHG can differ substantially from the total C budget (Drewer et al. 2010). As the methane production pathway has an effect on the isotopic composition of CH<sub>4</sub>, it also affects the evolution of DIC. An increase in  $\delta^{13}\text{C}_{\text{CH}_4}$  leads to a decrease in  $\delta^{13}\text{C}_{\text{DIC}}$  (Clark and Fritz 1997) and it is shown in Figures 16 and 17. The enrichment effect is not uniform and gives both methane production pathways distinctive fractioning factors between the two carbon compounds. For CO<sub>2</sub> reduction the fractioning factor  $\alpha^{13}\text{C}_{\text{CH}_4\text{-CO}_2}$  is empirically shown to be less than 0.935 and to acetate fermentation usually over 0.95 (Whiticar et al. 1986, Lansdown et al. 1992, Clark and Fritz 1997). Fractioning factors in between usually indicate combined production pathways.

Table 13 shows the fractioning factors  $\alpha^{13}\text{C}_{\text{CH}_4\text{-CO}_2}$  for each microsite per month. At the most microsites, ruling production pathway cannot be clearly identified. However, the bog shows more tendencies to CO<sub>2</sub> reduction and the fen to acetate fermentation. Since this study did not contain pore water samples of  $\delta^{13}\text{C}_{\text{CH}_4}$  from the same depth than the DIC samples were collected, the data cannot be used to identify methane production pathways with certainty by calculating fractioning factors. Nevertheless, some interpretation can still be made, as other studies indicate that the emitted methane has similar isotopic composition than CH<sub>4</sub> at the depth of 1 m (Dorodnikov et al. 2013) and the isotopic composition of DIC does not change significantly between 0.5–1.0 m (Chasar et al. 2000b).

Table 13. Fractioning factors  $\alpha^{13}\text{C}_{\text{CH}_4\text{-CO}_2}$  to determine methane production pathways at each sampled microsite.

	$\alpha^{13}\text{C}_{\text{CH}_4\text{-CO}_2} / \text{Bog}$				$\alpha^{13}\text{C}_{\text{CH}_4\text{-CO}_2} / \text{Fen}$		
	HO	HL	HHU		HO	CR	HHU
May	0.94	0.94	0.94	May	0.96	0.95	0.94
July	0.93	0.93	0.93	July	0.94	0.94	0.95
August	0.94	0.93	0.94	August	0.94	0.95	0.94

$\delta^{13}\text{C}_{\text{DIC}}$  is significantly more negative at the fen than at the bog owing to the differences in nutrient status, pH, vegetation, and thus higher amount of acetate fermentation. In May, the  $\delta^{13}\text{C}_{\text{DIC}}$  from hollows and *Carex* lawns was close to the isotopic composition of groundwater and precipitation in Finland (Kortelainen 2007), indicating that there was less methanogenesis in the beginning of the growing period. The difference between microsites is widest at early in the growing season and narrows down towards end of the season, and the monthly variation at the fen is more drastic than at the bog. Chasar et al. (2000b) reported same magnitude difference between bog and fen, at the depth of 0.5 m, at Minnesota peatland in July that this data showed in May.

At the bog the mean DIC values showed enrichment of approx. 3 ‰ during the growing period and at the fen the enrichment was approx. 9 ‰. Enrichment during the growing period can be explained with development of vascular plants, as growing plant production favours lighter isotopes and heavier isotopes are dissolved to pore water in greater portion. The higher variation at the fen could be derived from low substrate availability in high and late summer, supporting the independence of  $\text{CH}_4$  emissions from peat temperature.

At both sites, the DIC values showed also a significant variation between microsites. At the bog, the trend of most negative  $\delta^{13}\text{C}$  values at hummocks is obvious, which is derived from the level of  $\text{CH}_4$  oxidations as it shows as depletion in  $\delta^{13}\text{C}_{\text{DIC}}$  values (Barker and Fritz 1981). At the fen, DIC shows less dependency on microtopography, as each month a different microsite depicts most negative value. The mean DIC values from microsites shows most enriched  $\delta^{13}\text{C}$  from hummocks, which is opposite to the

bog, owing to the emphasized role of produced  $\text{CH}_4$  gas bypassing oxidation via vascular plants.

## 7. CONCLUSION

The results from the Siikaneva bog and fen indicate complex interactions in methane production, transport and oxidation, resulting in high spatial and temporal variations both within and between peatland ecosystems. With this in mind, the following concluding remarks can be drawn.

At Siikaneva, the bog and the fen act mainly as sources of atmospheric methane during the growing period. Only the hummocks on the fen (at the end of the summer) display high enough oxidation to act as sinks of atmospheric methane. Total summertime  $\text{CH}_4$  emissions were measured to be marginally greater for the bog than those for the fen, in contrast to general observations.

Different microsite types affect  $\text{CH}_4$  emission rates and have separable effects on the isotope composition of carbon in the emitted  $\text{CH}_4$  and pore water DIC. For the flux, hummocks display lower rates than hollows, but lawns are not distinguished clearly from the other microsites. The differences between microsites are more concordant with microtopography on the bog than on the fen. Hence, microtopography only seems to function as an indicator of flux within a more homogenous ecosystem and prefers distinctive variation in elevation.  $\text{CH}_4$  emissions do not show large scale correlation with water table position or peat temperature.

The isotopic composition of emitted methane is more negative at the bog than at the fen. However, the difference in the  $\delta^{13}\text{C}_{\text{CH}_4}$  values between the bog and the fen is more subtle and less indicative than anticipated in the hypothesis. On the bog, microtopography affects the isotopic composition of emitted  $\text{CH}_4$  and pore water DIC, as hummocks have more enriched  $^{13}\text{C}_{\text{CH}_4}$  and depleted  $^{13}\text{C}_{\text{DIC}}$  values than hollows and lawns. On the fen,  $\delta^{13}\text{C}_{\text{CH}_4}$  and  $\delta^{13}\text{C}_{\text{DIC}}$  values are less systematically affected by microtopography. The mean of  $^{13}\text{C}_{\text{DIC}}$  enriched towards the end of the summer, and the enrichment was more pronounced on the fen, likely due to the increased rate of



methanogenesis via acetate fermentation pathway. Methane production pathway is not unambiguous, as methane is produced via two pathways, but the results suggest that the bog has more CO<sub>2</sub> reduction than the fen.

The  $\delta^{13}\text{C}_{\text{CH}_4}$  values from the emissions alone are not sufficient to identify the methanogenic pathway of CH<sub>4</sub> production with certainty. In order to draw conclusions of production pathways, pore water isotope samples for  $\delta^{13}\text{C}_{\text{DIC}}$  and  $\delta^{13}\text{C}_{\text{CH}_4}$  analyses should be drawn from multiple depths to demonstrate the vertical changes in isotope composition at different layers of peat, and to distinguish seasonal patterns at different microsites.

## **8. ACKNOWLEDGEMENTS**

This master's project has proved to be an interesting journey with its ups and downs. I would like to thank my supervisors Professor Juha Karhu and Professor Janne Rinne for teaching and guiding me through the process. I thank Salli Uljas for showing me the sites and the basics of chamber measurements, and Matti Lopenen for analysing my concentration samples at Hyytiälä. I would also like to thank Paula Niinikoski for teaching me the DIC analysis and for valuable lab assistance whenever the IRMS was having a bad day. I sincerely appreciated the guiding comments from Aino Korrensalo when I was feeling unsure with my flux data. For financial support and internship related to this project, I would like to acknowledge Department of Physics, University of Helsinki.

My deepest gratitude goes to my family and friends for the loving support you give me every day. Markus, without you I would be lost. And I'm not just referring to the nighttime field campaign, where I was so lucky to have you by my side. Vilho, I thank you so much for your unconditional support. I know it hasn't been easy to play police car chase with a minimal amount of sounds, but you performed perfectly.

## 9. REFERENCES

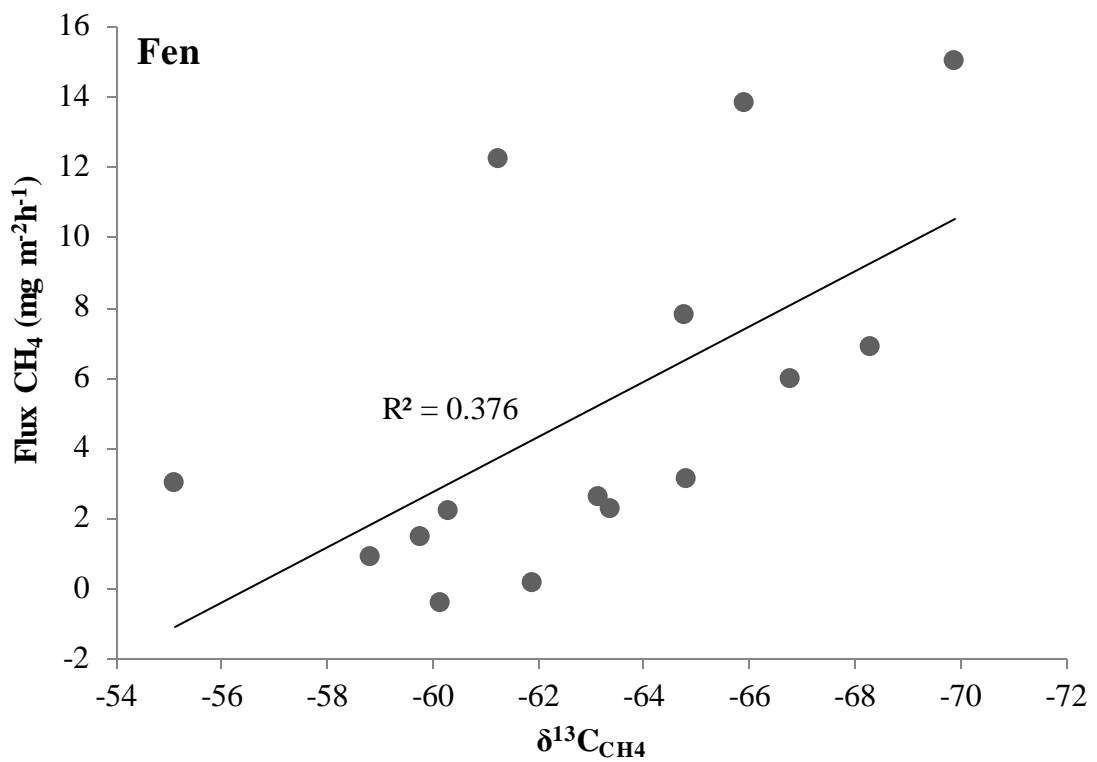
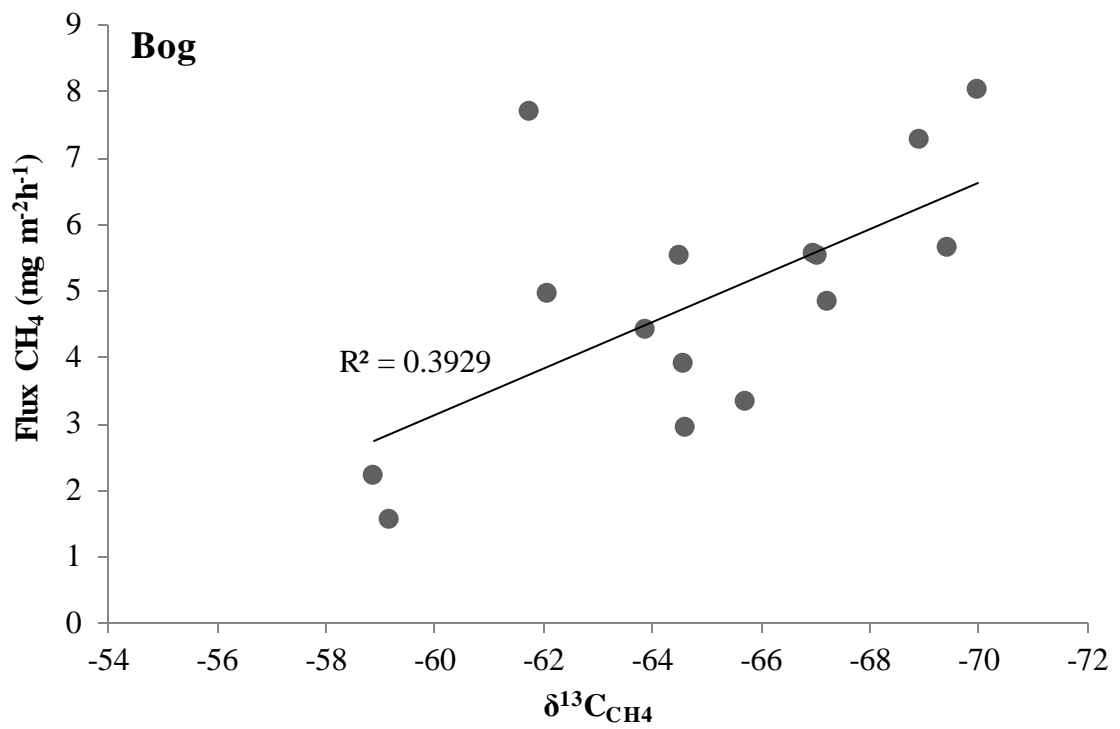
- Ahti, T., Hämet-Ahti, L. and Jalas, J. 1968. Vegetation zones and their sections in northwestern Europe. *Annales Botanici Fennici*, 5, 169–211.
- Alanen, A. and Aapala, K. 2015. Soidensuojelutyöryhmän ehdotus soidensuojelun täydentämiseksi. Ympäristöministeriön raportteja, 26. 178 p.
- Aurela, M., Riutta, T., Laurila, T., Tuovinen, J., Vesala, T., Tuittila, E., Rinne, J., Haapanala, S. and Laine, J. 2007. CO<sub>2</sub> exchange of a sedge fen in southern Finland—the impact of a drought period. *Tellus*, 59B, 826–837.
- Aurela, M., Lohila, A., Tuovinen, J., Hatakka, J., Riutta, T. and Laurila, T. 2009. Carbon dioxide exchange on a northern boreal fen. *Boreal environment research*, 14, 699–710.
- Barker, J. and Fritz, P. 1981. Carbon isotope fractionation during microbial methane oxidation. *Nature*, 293, 289–291.
- Becker, T., Kutzbach, L., Forbrich, I., Schneider, J., Jäger, D., Thees, B. and Wilmking, M. 2008. Do we miss the hot spots? – The use of very high resolution aerial photographs to quantify carbon fluxes in peatlands. *Biogeosciences*, 5, 1387–1393.
- Bellisario, L., Bubier, J., Moore, T. and Chanton J. 1999. Controls on CH<sub>4</sub> emissions from a northern peatland. *Global Biogeochemical Cycles*, 13, 81–91.
- Bowes, H. and Hornibrook, E. 2006. Emissions of highly <sup>13</sup>C-depleted methane from an upland blanket bog. *Geophysical Research Letters*, 33, L04401.
- Brown, D. 1998. Gas production from an ombrotrophic bog - effect of climate change on microbial ecology. *Climatic Change*, 40, 277–284.
- Bubier, J. 1995. The relationship of vegetation to methane emission and hydrochemical gradients in northern peatlands. *Journal of Ecology*, 83, 403–420.
- Chanton, J., Bauer, J., Glaser, P., Siegel, D., Kelley, C., Tyler, S., Romanowicz, E. and Lazrus, A. 1995. Radiocarbon evidence for the substrates supporting methane formation within northern Minnesota peatlands. *Geochimica et Cosmochimica Acta*, 59, 3663–3668.
- Chanton, J., Arkebauer, T., Harden, H. and Verma, S. 2002. Diel variation in lacunal CH<sub>4</sub> and CO<sub>2</sub> concentration and δ<sup>13</sup>C in *Phragmites australis*. *Biogeochemistry*, 59, 287–301.
- Chanton, J., Chasar, L., Glaser, P. and Siegel, D. 2005. Carbon and Hydrogen Isotopic Effects in Microbial Methane from terrestrial Environments. In: Flanagan, L., Ehleringer, J. and Pataki, D. (eds.) *Stable Isotopes and Biosphere-Atmosphere Interactions*. Elsevier-Academic, Amsterdam, 85–105.
- Chapellaz, J., Barnola, J., Raynaud, D., Korotkevich, Y. and Lorius, C. 1990. Ice-core Record of Atmospheric Methane over the past 160,000 years. *Nature*, 345, 127–131.
- Chasar, L., Chanton, P., Glaser, P. and Siegel, D. 2000a. Methane concentration and stable isotope distribution as evidence of rhizospheric processes: Comparison of a fen and bog in the Glacial Lake Agassiz Peatland complex. *Annals of Botany*, 86, 655–663.
- Chasar, L., Chanton, P., Glaser, P., Siegel, D. and Rivers, S. 2000b. Radiocarbon and stable carbon isotopic evidence for transport and transformation of dissolved organic carbon, dissolved inorganic carbon, and CH<sub>4</sub> in a northern Minnesota peatland. *Global Biogeochemical Cycles*, 14, 1095–1108.
- Christensen, T., Ekberg, A., Ström, L., Mastepanov, M., Panikov, N., Öquist, M., Svensson, B., Nykänen, H., Martikainen, P. and Oskarsson, H. 2003a. Factors controlling large scale variations in methane emissions from wetlands. *Geophysical Research Letters*, 30, 1414, DOI:2003GL016848.
- Christensen, T., Panikov, N., Mastepanov, M., Joabsson, A., Stewart, A., Öquist, M., Sommerkorn, M., Reynaud, S. and Svensson, B. 2003b. Biotic controls on CO<sub>2</sub> and CH<sub>4</sub> exchange in wetlands—a closed environment study. *Biogeochemistry*, 64, 337–354.

- Clark, I. and Fritz, P. 1997. Environmental isotopes in hydrogeology. CRC Press, Washington, 342 p.
- Clymo, R. 1984. The limits to Peat Bog Growth. Philosophical Transactions Royal Society London B, 303, 605–654.
- Crill, P., Bartlett, K. and Roulet, N. 1993. Methane flux from boreal peatlands. *Suo*, 43, 173–182.
- Davidson, E., Savage, K., Verchot, L. and Navarro, R. 2002. Minimizing artifacts and biases in chamber-based measurements of soil respiration. *Agricultural and Forest Meteorology*, 113, 21–37.
- Ding, W., Cai, Z. and Tsuruta, H. 2004. Methane concentration and emission as affected by methane transport capacity of plants in freshwater marsh. *Water, Air & Soil Pollution*, 158, 99–111.
- Dlugokencky, E., Bruhwiler, L., White, J., Emmons, L., Novelli, P., Montzka, S., Masarie, K., Lang, P., Crotwell, A., Miller, J. and Gatti L. 2009. Observational constraints on recent increases in the atmospheric CH<sub>4</sub> burden. *Geophysical Research Letters*, 36, L18803.
- Dorodnikov, M., Marushchak, M., Biasi, C., and Wilmking, M. 2013. Effect of microtopography on isotopic composition of methane in porewater and efflux at a boreal peatland, *Boreal Environmental Research*, 18, 269–279.
- Drewer, J., Lohila, A., Aurela, M., Laurila, T., Minkinen, K., Penttilä, T., Dinsmore, K., McKenzie, R., Helfter, C., Flechard, C., Sutton, M. and Skiba, U. 2010. Comparison of greenhouse gas fluxes and nitrogen budgets from an ombrotrophic bog in Scotland and a minerotrophic sedge fen in Finland. *European Journal of Soil Science*, 61, 640–650.
- Galand, P., Fritze, H., Conrad, R. and Yrjälä, K. Pathways for methanogenesis and diversity of methanogenic Archaea in three boreal peatland ecosystems. *Applied and Environmental Microbiology*, 71, 2195–2198.
- Gerard, G. and Chanton, J. 1993. Quantification of methane oxidation in the rhizosphere of emergent aquatic macrophytes - Defining upper limits. *Biogeochemistry*, 23, 79–97.
- Gorham, E. 1991. Northern Peatlands: Role in the Carbon Cycle and Probable Responses to Climatic Warming. *Ecological Applications*, 1, 182–195.
- Hanson, R. and Hanson, T. 1996. Methanotrophic bacteria. *Microbiological Reviews*, 60, 439–471.
- Heikkinen, J., Maljanen, M., Aurela, M., Hargreaves, K. and Martikainen, P. 2002. Carbon dioxide and methane dynamics in a sub-Arctic peatland in northern Finland. *Polar Research*, 21, 49–62.
- Horita, J. and Berndt, M. 1999. Abiogenic Methane Formation and Isotopic Fractionation Under Hydrothermal Conditions. *Science*, 13, 1055–1057.
- Horn, M., Matthies, C., Kusel, K., Schramm, A. and Drake, H. 2003. Hydrogenotrophic methanogenesis by moderately acid-tolerant methanogens of a methane-emitting acidic peat. *Applied and Environmental Microbiology*, 69 (1), 74–83.
- Hornibrook, E. 2009. The stable carbon isotope composition of methane produced and emitted from northern peatlands. In: Baird, A., Belyea, L., Comas, X., Reeve, A. and Slater, L. (eds.) *Carbon Cycling in Northern Peatlands*. AGU. Washington. 299 p.
- Hornibrook, E. and Bowes, H. 2007. Trophic status impacts both the magnitude and stable carbon isotope composition of methane flux from peatlands. *Geophysical Research Letters*, 34, L21401.
- Hornibrook, E., Longstaffe, F. and Fyfe, W. 1997. Spatial distribution of microbial methane production pathways in temperate zone wetland soils: Stable carbon and hydrogen isotope evidence. *Geochimica et Cosmochimica Acta*, 61, 745–753.
- IPCC (Intergovernmental Panel on Climate Change). 2013. *Climate Change 2013. The Physical Science Basis. Summary for Policymakers*. Switzerland.
- Kamal, S. and Varma, A. 2008. Peatland microbiology. In: Dion, P. and Nautiyal, C. (eds.) *Microbiology of Extreme Soils. Soil Biology 13*. Springer-Verlag, Berlin Heidelberg. 177–203.
- Keeling, C. 1961. The concentration and isotopic abundance of carbon dioxide in rural and marine air. *Geochimica et Cosmochimica Acta*, 24, 277–298.

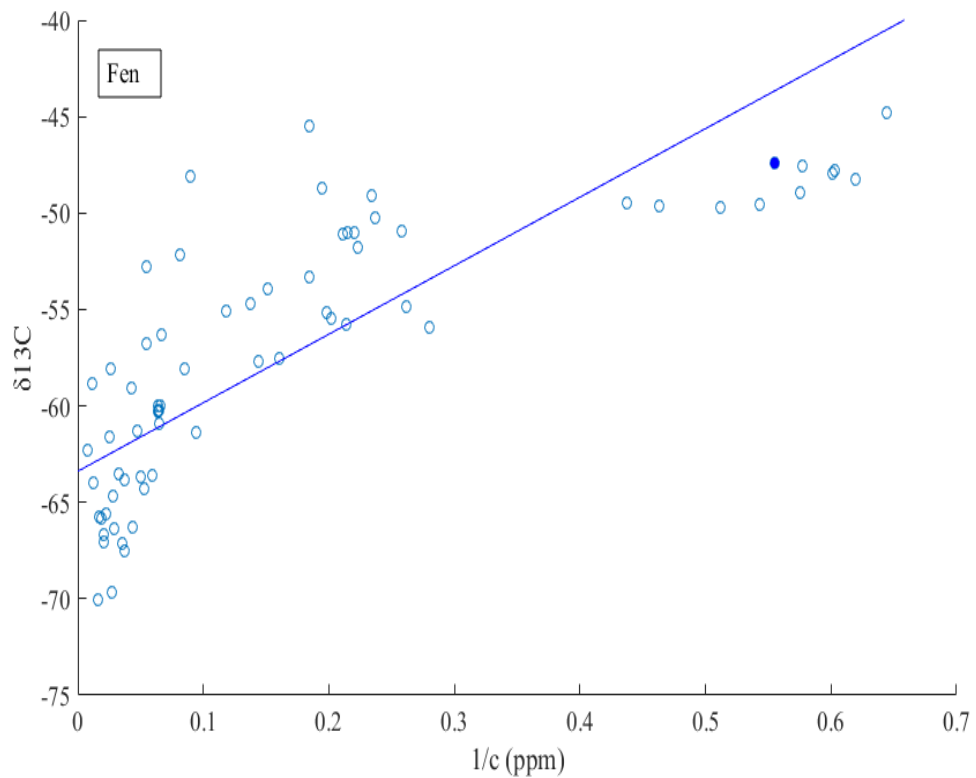
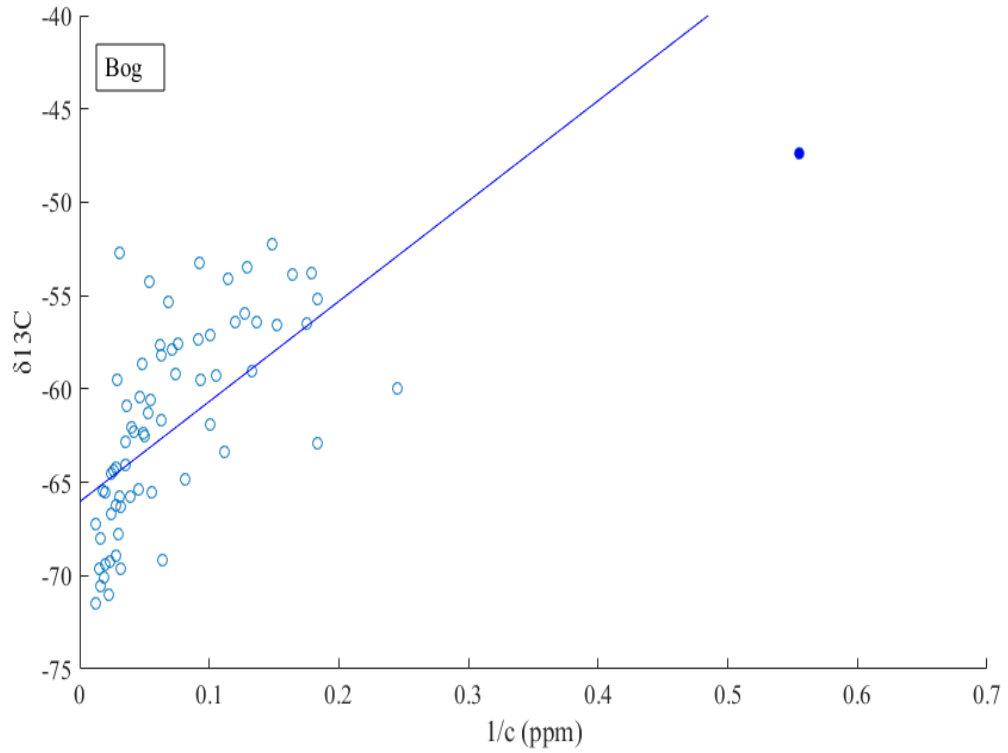
- Kohn, M. 2010. Carbon isotope compositions of terrestrial C3 plants as indicators of (paleo)ecology and (paleo)climate. *Proceedings of the National Academy of Sciences*, 107, 19691–19695.
- Korhola, A. and Tolonen, K. 1998. Suomen soiden kehityshistoria ja turpeen pitkäaikauskertymät. In: Vasander, H. (eds.) *Suomen suot*. Suoseura ry. Helsinki. 168 p.
- Kortelainen, N. 2007. Isotopic Fingerprints In Surficial Waters: Stable Isotope Methods Applied In Hydrogeological Studies. PhD-thesis No. 199 of the Department of Geology, University of Helsinki.
- Lai, D. 2009. Methane dynamics in Northern peatlands: A review. *Pedosphere*, 19(4), 409–421.
- Laine, J. and Vasander H. 1998. Suon määritelmiä ja käsitteitä. In: Vasander, H. (eds.) *Suomen suot*. Suoseura ry. Helsinki. 168 p.
- Lansdown, J. 1992. CH<sub>4</sub> production via CO<sub>2</sub> reduction in a temperate bog: A source of <sup>13</sup>C-depleted CH<sub>4</sub>. *Geochimica et Cosmochimica Acta*, 56, 3493–3503.
- Lashof, D. and Ahuja, D. 1990. Relative contributions of greenhouse gas emissions to global warming. *Nature*, 344, 529–531.
- Legendre, P. 2013. Model II regression user's guide, R edition. <https://cran.rproject.org/web/packages/lmodel2/vignettes/mod2user.pdf>. Page visited 26.6.2016.
- Loulergue, L., Schilt, A., Spahni, R., Masson-Delmotte, V., Blunier, T., Lemieux, B., Barnola, J., Raynaud, D., Stocker, T. and Chappellaz, J. 2008. Orbital and millennial-scale features of atmospheric CH<sub>4</sub> over the past 800,000 years. *Nature*, 453, 383–386.
- MacDonald, J., Fowler, D., Hargreaves, K., Skiba, U., Leith, I. and Murray, M. 1998. Methane emission rates from a northern wetland; response to temperature, water table and transport. *Atmospheric Environment*, 32, 3219–3227.
- Mikkilä, C., Sundh, I., Svensson, B. and Nilsson, M. 1995. Diurnal Variation in Methane Emission in Relation to the Water Table, Soil Temperature, Climate and Vegetation Cover in a Swedish Acid Mire. *Biogeochemistry*, 28, 93–111.
- Minkinen, K., Korhonen, R., Savolainen, I. and Laine, J. 2002. Carbon balance and radiative forcing of Finnish peatlands 1900-2100 - the impact of forestry drainage. *Global Change Biology*, 8, 785–799.
- Moore, T. and Basilisko, N. 2006. Decomposition in boreal peatlands. In: Wieder, K. and Vitt, D. (eds.) *Boreal Peatland Ecosystems*. Springer Berlin Heidelberg. 125–143.
- Moore, T. and Knowles, R. 1990. Methane emissions from fen, bog and swamp peatlands in Quebec. *Biogeochemistry* 11, 45–61.
- Moore, T. and Roulet, N. 1993. Methane flux: Water table relations in northern wetlands. *Geophysical Research Letters*, 20, 587–590.
- Nykänen, H., Alm, J., Silvola, J., Tolonen, K. & Martikainen, P.J. 1998. Methane fluxes on boreal peatlands of different fertility and the effect of long-term experimental lowering of the water table on flux rates. *Global biogeochemical cycles*, 12, 53–69.
- Pataki, D., Ehleringer, J., Flanagan, L., Yakir, D., Bowling, D., Still, C., Buchmann, N., Kaplan, J. and Berry J. 2003. The application and interpretation of Keeling plots in terrestrial carbon cycle research. *Global Biogeochemical Cycles*, 17(1), 1022.
- Petit, J., Jouzel, J., Raynaud, D., Barkov, N., Barnola, J., Basile, I., Bender, M., Chappellaz, J., Davisk, M., Delaygue, G., Delmotte, M., Kotlyakov, V., Legrand, M., Lipenkov, V., Lorius, C., Pe'pin, L., Ritz, C., Saltzman, E. and Stevenard, M. 1999. Climate and Atmospheric History of the Past 420,000 years from the Vostok Ice Core, Antarctica. *Nature*, 399, 429–436.
- Pihlatie, M., Pumpanen, J., Rinne, J., Ilvesniemi, H., Simojoki, A., Hari, P. and Vesala, T. 2007. Gas concentration driven fluxes of nitrous oxide and carbon dioxide in boreal forest soil. *Tellus*, 59B, 458–469.
- Pirinen, P., Simola, H., Aalto, J., Kaukoranta, J., Karlsson, P. and Ruuhela R. 2012. Tilastoja Suomen ilmastosta 1981-2010. Ilmatieteenlaitoksen raportteja, 2012:1. 96p.
- Prather, M., Derwent, R., Ehhalt, D., Fraser, P., Sanhueza, E. and coauthors.

1995. Other trace gases and Atmospheric Chemistry. In: *Climate Change 1994, Radiative Forcing of Climate Change and Evaluation of the IPCC IS92 Emission Scenarios* (eds. Houghton, J and co-authors), Cambridge University Press, Cambridge, UK, 77–126.
- Quya, P., King, S., Lansdown, J. and Wilbur, D. 1988. Isotopic composition of methane released from wetlands: Implications for the increase in atmospheric methane. *Global Biogeochemical Cycles*, 2(4), 385–397.
- Rigby, M., Prinn, R., Fraser, P., Simmonds, P., Langenfelds, R., Huang, J., Cunnold, D., Steele, L., Krummel, P., Weiss, R., O'Doherty, S., Salameh, P., Wang, H., Harth, C., Mühle, J. and Porter L. 2008. Renewed growth of atmospheric methane. *Geophysical Research Letters*, 35, L22805
- Rinne, J., Riutta, T., Pihlatie, M., Aurela, M., Haapanala, S., Tuovinen, J., Tuittila, E. and Vesala, T. 2007. *Tellus*, 59B, 449–457.
- Riutta, T., Laine, J., Aurela, M., Rinne, J., Vesala, T., Laurila, T., Haapanala, S., Pihlatie, M. and Tuittila, E. 2007. *Tellus*, 59B, 838–852.
- Rydin, H. and Jeglum, J. 2006. *The Biology of Peatlands*. OUP, Oxford. 354 p.
- Saarnio, S., Alm, J., Silvola, J., Lohila, A., Nykänen, H. and Martikainen P. 1997. Seasonal Variation in CH<sub>4</sub> Emissions and Production and Oxidation Potentials at Microsites on an Oligotrophic Pine Fen. *Oecologia*, 110, 414–422.
- Segers, R. 1998. Methane production and methane consumption: A review of processes underlying wetland methane fluxes. *Biogeochemistry*, 41, 23–51.
- Silvan, N., Saarinen, M., Sarkkola, S., Päivänen, J. and Vasander, H. 2008. Siikaneva – Pirkanmaan laajin suoerämaa. Publications from the Department of Forest Ecology, University of Helsinki, 37, 1–88.
- Sokal, R., and Rohlf, F. 1995. *Biometry*. W. H. Freeman. New York.
- Sriskantharajah, S., Fisher, R., Lowry, D., Aalto, T., Hatakka, J., Aurela, M., Laurila, T., Lohila, A., Kuitunen, E. and Nisbet, E. 2012. Stable carbon isotope signatures of methane from a Finnish subarctic wetland. *Tellus*, 64B, 18818.
- Stevens, C. and Walen, M. 2000. The Isotopic Composition of Atmospheric Methane and Its Sources. In: Khalil, M. (eds.) *Atmospheric Methane, Its Role in the Global Environment*. Springer Berlin Heidelberg. 25–41.
- Thermo Scientific. 2013. *PreCon Operating Manual (P/N 1110050, Revision A)*.
- Tokida, T., Miyazaki, T., Mizoguchi, M., Nagata, O., Takakai, F., Kagemoto, A. and Hatano, R. 2007. Falling atmospheric pressure as a trigger for methane ebullition from peatland. *Global Biogeochemical Cycles*, 21, GB2003.
- Turunen, J., Tomppo, E., Tolonen, K. and Reinikainen, A. 2002. Estimating carbon accumulation rates of undrained mires in Finland – application to boreal and subarctic regions. *The Holocene*, 12 (1), 69–80.
- Uljas, S. 2015. Keidassuoekosysteemin kasviyhteisötyyppien hiilidioksidinvaihto. Master's theses, University of Eastern Finland, Department of Biology. 63 p.
- Whalen, S. 2005. Biochemistry of methane exchange between natural wetlands and the atmosphere. *Environmental Engineering Science*, 22 (1), 73–94.
- Whiticar, M. 1999. Carbon and hydrogen isotope systematics of bacterial formation and oxidation of methane. *Chemical Geology*, 161, 291–314.
- Whiticar, M., Faber, E. and Schoell, M. 1986. Biogenic methane formation in marine and freshwater environments: CO<sub>2</sub> reduction vs. acetate fermentation - Isotopic evidence. *Geochimica et Cosmochimica Acta*, 50, 693–709.
- Whiting, G. and Chanton, J. 1993. Primary production control of methane emission from wetlands. *Nature*, 364, 794–795.

Appendix 1. Average fluxes in relation to average  $\delta^{13}\text{C}_{\text{CH}_4}$  values at both sites.



Appendix 2. The Keeling plots for both sites depicting all isotope results. On the bog, the average source signature (intercept) is  $-66.0 \pm 0.7 \text{ ‰}$  ( $R^2 = 0.70$ ). On the fen, the average source signature is  $-63.2 \pm 0.8 \text{ ‰}$  ( $R^2 = 0.77$ ).



Appendix 3. The Keeling plot source signatures and flux measurements from each microsite. Isotope source signature is the intercept of y-axis in the Keeling plot linear regression. The uncertainty is the standard error in the intercept.  $R^2$  is the correlation coefficient between  $\text{CH}_4$  concentration and  $\delta^{13}\text{C}$ .

Bog		Source signature				Flux measurements				
Month	Microsite	$\delta^{13}\text{C}$ (‰)	SE $\pm$ (‰)	$R^2$	n	Mean ( $\text{mg m}^{-2}\text{h}^{-1}$ )	SD	Min	Max	n
May	HO	-62.07	1.21	0.93	6	4.9	5.0	1.4	8.5	2
	HL	-63.89	0.49	0.99	4	4.4	1.5	3.1	6.0	3
	HHU	-58.87	1.78	0.83	5	2.2	1.3	0.7	3.1	3
June	HO	-67.04	1.92	0.88	6	5.5	1.8	3.4	6.8	3
	HL	-67.24	1.39	0.93	6	4.8	0.6	4.3	5.4	3
	HHU	-59.16	1.10	0.90	6	1.5	1.2	0.6	2.8	3
July	HO	-69.99	0.70	0.99	4	8.0	1.1	6.7	8.7	3
	HL	-66.96	2.52	0.90	4	5.5	4.4	1.7	10.4	3
	HHU	-64.62	3.43	0.72	5	2.9	0.6	2.3	3.5	3
August	HO	-64.56	2.55	0.82	5	3.9	4.2	1.2	8.7	3
	HL	-65.70	1.85	0.87	6	3.3	2.6	0.9	6.1	3
	HHU	-61.73	2.73	0.71	6	7.7	1.1	6.6	8.7	3
August night	HO	-69.44	1.73	0.99	2	5.6	-	-	-	1
	HL	-64.51	0.68	1.00	2	5.5	-	-	-	1
	HHU	-68.90	-	-	1	7.3	-	-	-	1

Fen		Source signatures per month				Flux measurements				
Month	Microsite	$\delta^{13}\text{C}$ (‰)	SE $\pm$ (‰)	$R^2$	n	Mean ( $\text{mg m}^{-2}\text{h}^{-1}$ )	SD	Min	Max	n
May	HO	-60.32	2.37	0.81	5	2.2	0.8	1.6	3.0	3
	CR	-59.78	2.07	0.84	5	1.4	0.4	1.0	1.7	3
	HU	-64.79	4.08	0.87	4	7.8	10.9	0.1	15.4	2
June	HO	-64.83	1.25	0.93	6	3.1	0.6	2.4	3.4	3
	CR	-63.14	1.70	0.87	6	2.6	0.7	1.9	3.2	3
	HU	-58.84	2.07	0.83	6	0.9	-	-	-	1
July	HO	-65.75	4.68	0.71	4	6.9	1.1	5.8	7.9	3
	CR	-63.39	0.94	0.98	4	2.2	0.2	2.0	2.4	3
	HU	-61.89	4.78	0.72	6	0.1	0.2	-0.1	0.3	3
August	HO	-61.26	0.78	0.95	6	12.2	4.5	9.4	17.4	3
	CR	-55.12	2.20	0.54	6	3.0	0.0	2.9	3.0	3
	HU	-60.17	7.89	0.15	4	-0.4	0.2	-0.5	-0.3	2
August night	HO	-65.92	1.52	0.99	2	13.7	-	-	-	1
	CR	-69.90	0.87	1.00	2	15.0	-	-	-	1
	HU	-66.77	1.15	0.99	2	5.9	-	-	-	1